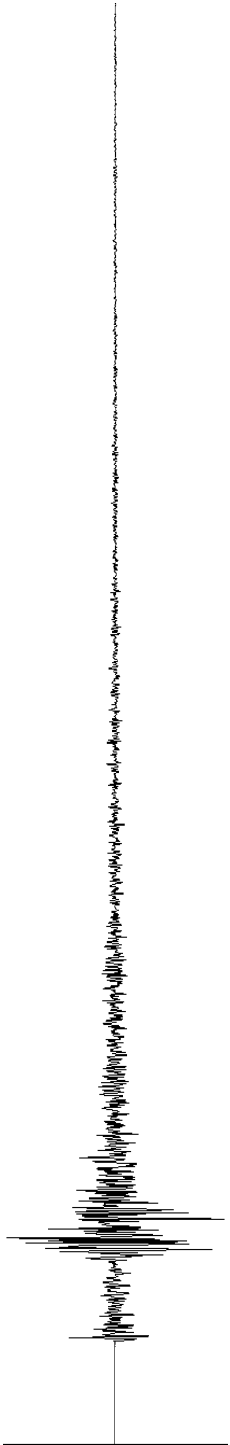


Inversion of local waveform data

- ✓ Peter Suhadolc
- ✓ Department of Earth
Sciences
- ✓ University of Trieste



Introduction

Solution of an inverse problem is required to interpret any measurements that are **indirect** like inferences of the properties of the Earth's interior and of the seismic source.

The basic measurements of seismology are, in fact, arrival times and amplitudes of different phases, or better, time series of ground motion. These data are controlled by both the elastic and inelastic properties of the Earth, as well as the properties of the source exciting the Earth. Inversion is a formal way to make inferences about these properties.



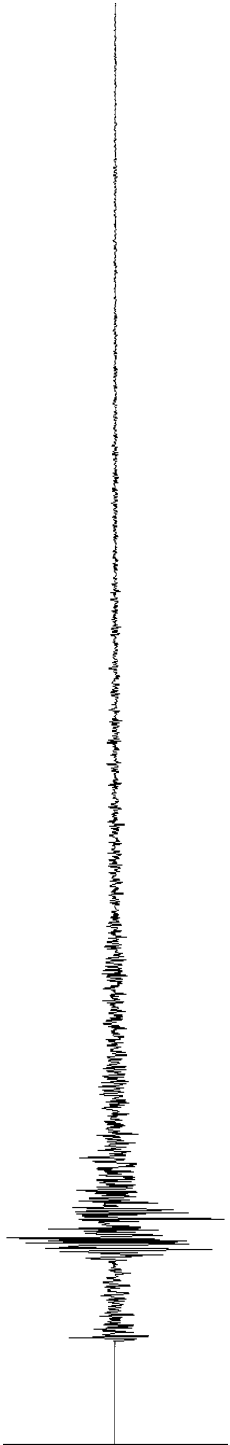
Introduction

The zeroth-order requirement for solution of any inverse problem is that before one can hope to solve the inverse problem, one has to be able to solve the "forward problem". This means that one has to understand the physical processes that produced the observation well enough to make a reliable mathematical model of the process.

The forward problem can be written schematically as

$$d_i = F_i [m(r)]$$

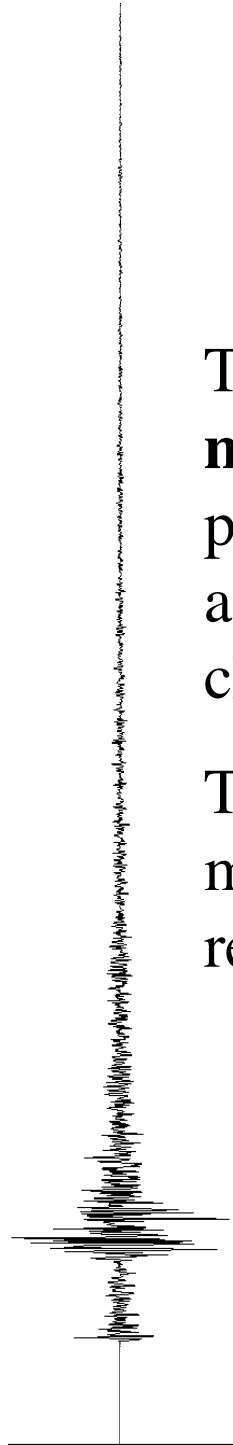
where $m(r)$ is a model describing some physical property of the Earth, d_i is the predicted value for datum i and F_i is a functional whose existence implies that if we know m exactly, we could predict the data perfectly.



Introduction

This is the simplest class of inverse solutions, the **forward modelling**, involving an educated guess (or a trial and error procedure) to derive an m that fits all the observable data according to some defined measure of goodness of fit (e.g., a chi-square test, minimum fit according to some norm etc.).

The fundamental **weakness** of this procedure is that once a model is found that fits the data, one does not know how reliable that model is.



Introduction

The fundamental difference between the construction of an inverse procedure compared to forward modelling is that the data are used directly to construct a solution. We can write this formally as:

$$m(r) = F_i^{-1} [d_i]$$

Every inverse problem should address the following aspects:

Existence: Does any model fit the data?

Uniqueness: Can the data uniquely constrain the model?

Construction: How can we find a solution?

Appraisal: How well do the data constrain the model.

Introduction

Existence: Does any model fit the data?

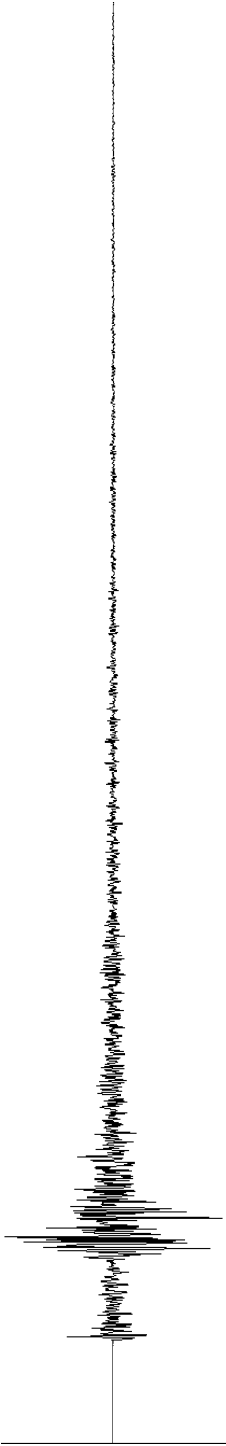
Uniqueness: Can the data uniquely constrain the model?

Construction: How can we find a solution?

Appraisal: How well do the data constrain the model.

Usually little attention is paid to the first two and much of the efforts go to the third aspect, the construction. Sometimes even the fourth aspect is neglected, which should be the most significant feature of a good inverse procedure. It answers the question of how good the solution one constructs really is.

In fact, finding a solution means nothing. The focus of a good analysis must lie with appraising the non-uniqueness of the solution.

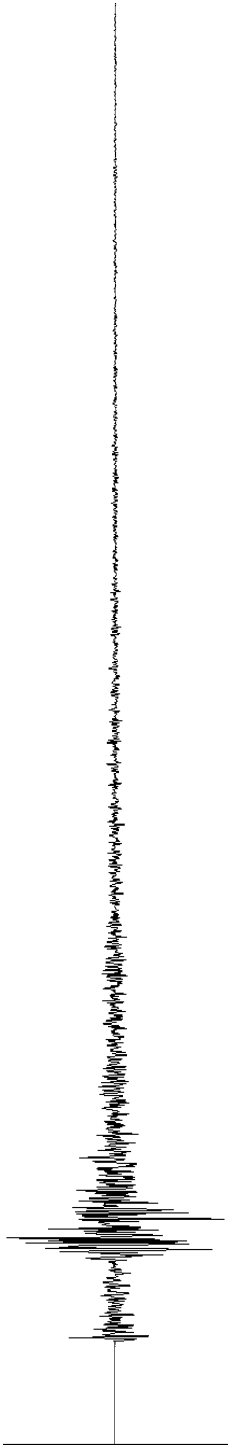


Introduction

Definition of some common terms used in inverse theory

STABILITY

Is defined as the property that a solution is insensitive to small random errors in the data

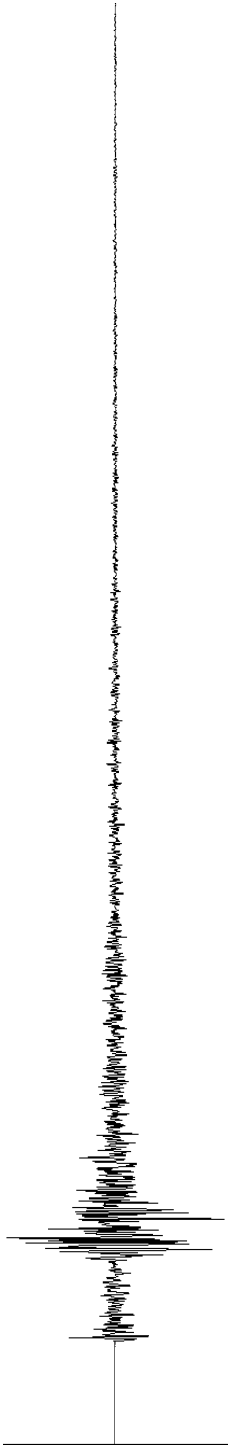


Introduction

Definition of some common terms used in inverse theory

ROBUSTNESS

Is the property that a solution is insensitive with respect to a small number of big errors (outliers) in the data

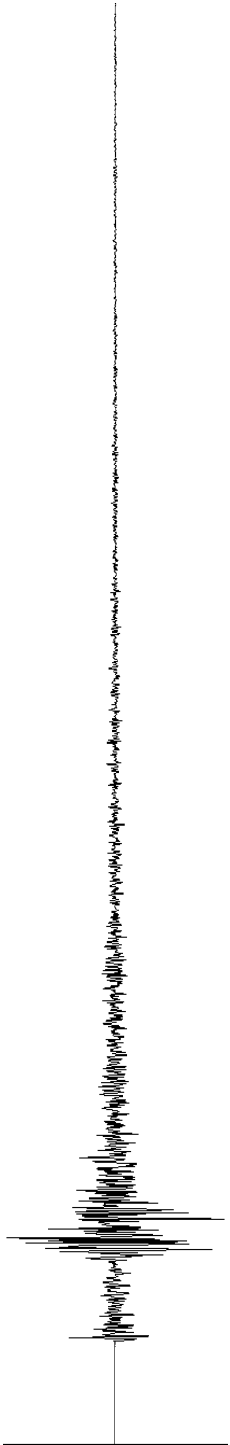


Introduction

Definition of some common terms used in inverse theory

NON-UNIQUENESS

Is the property that more than one solution (almost) equally well-fitting the data exists

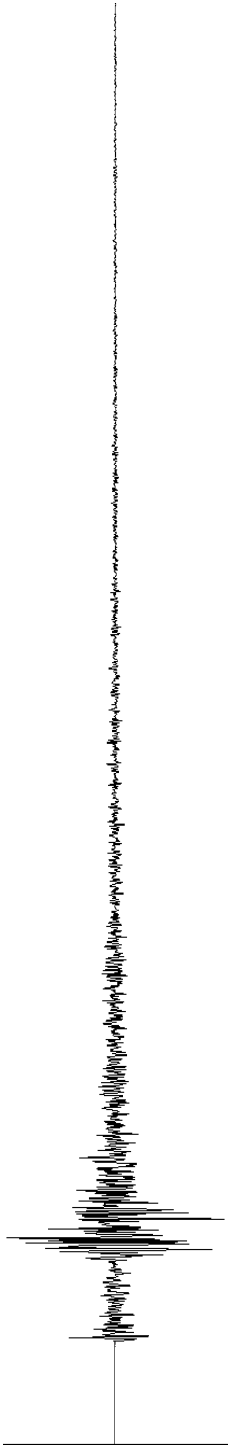


Introduction

Definition of some common terms used in inverse theory

GEOPHYSICS

In geophysics, the data itself contains noise and the models are themselves approximations

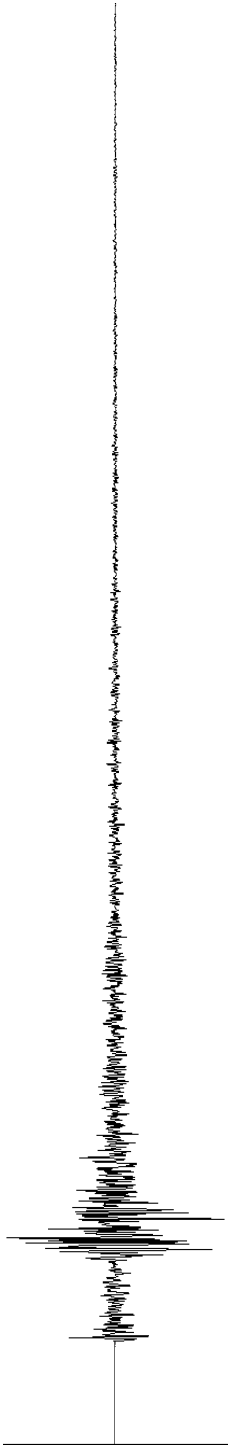


Introduction

Definition of some common terms used in inverse theory

UNSTABILITY

The inverse problem of obtaining the details of the rupture process from an analysis of recorded seismograms is an UNSTABLE problem

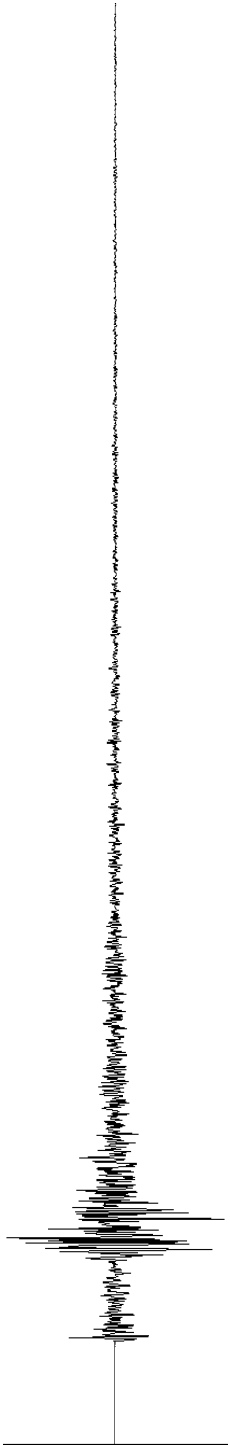


Introduction

Definition of some common terms used in inverse
theory

UNSTABILITY

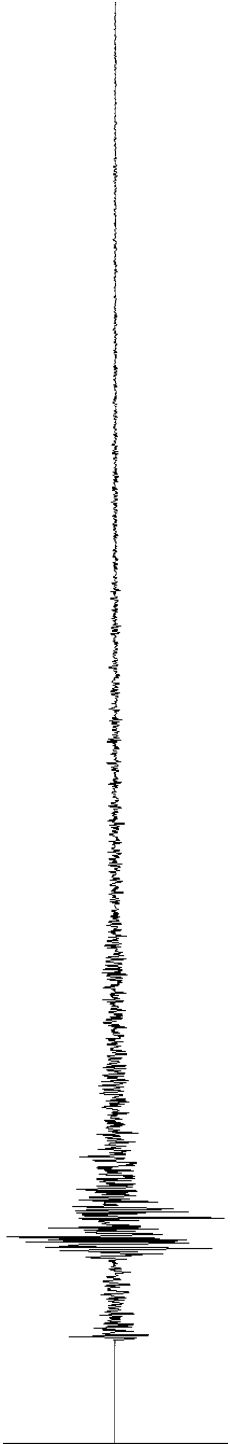
Note that the problem is unstable even in the imaginary case of a **continuous** distribution of seismic stations over the surface of the earth. From the computational point of view, the instability is equivalent to **non-uniqueness** of the solution.



Introduction

Definition of some common terms used in inverse theory

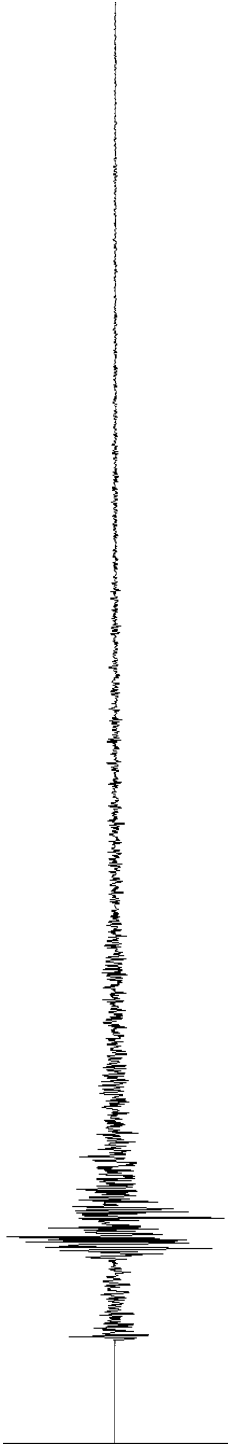
The **real** situation is even **worse** because the number of stations with appropriate records is very limited even today (5-10 in the local and regional case, 10-20 in the teleseismic case)



Introduction

Definition of some common terms used in inverse theory

Hence, one needs some **additional constraints** on the solution (i.e in addition to the requirement of fitting the seismograms). These constraints should be based on the **physics** of the earthquake faulting problem.

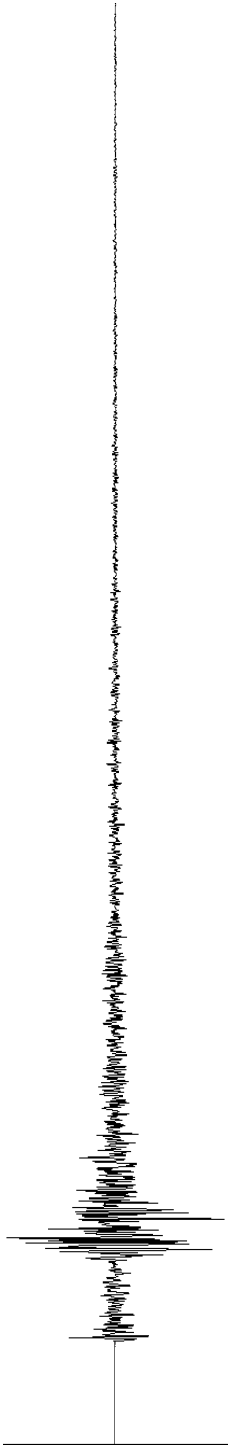


Inversion methods

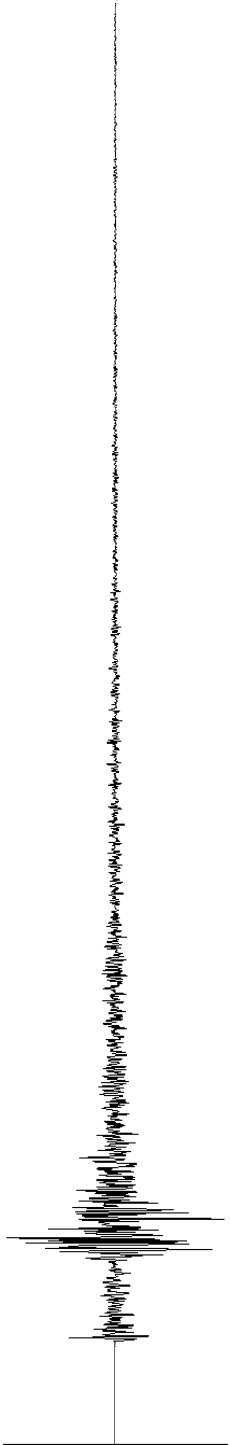
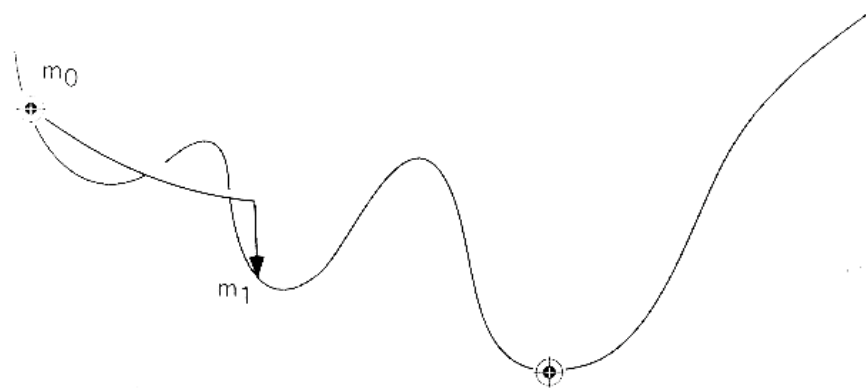
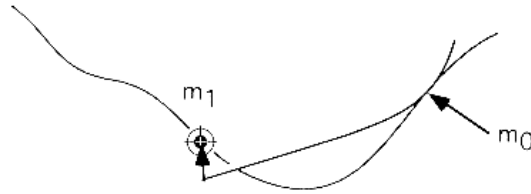
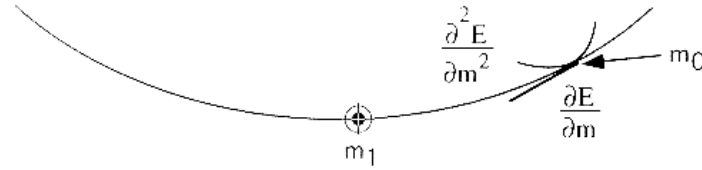
Downhill simplex method

Local search method, performs well if
local model is suitable

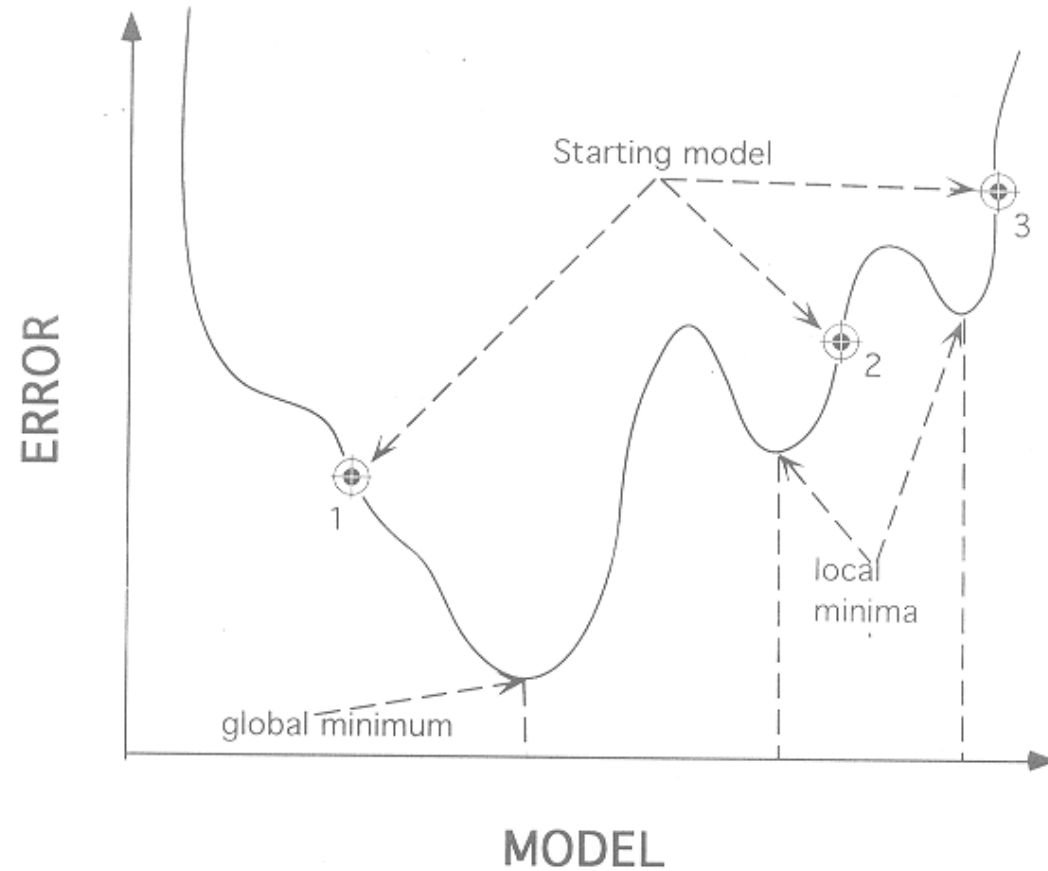
Nelder and Mead, 1965: Comput. J., 7, 308-313



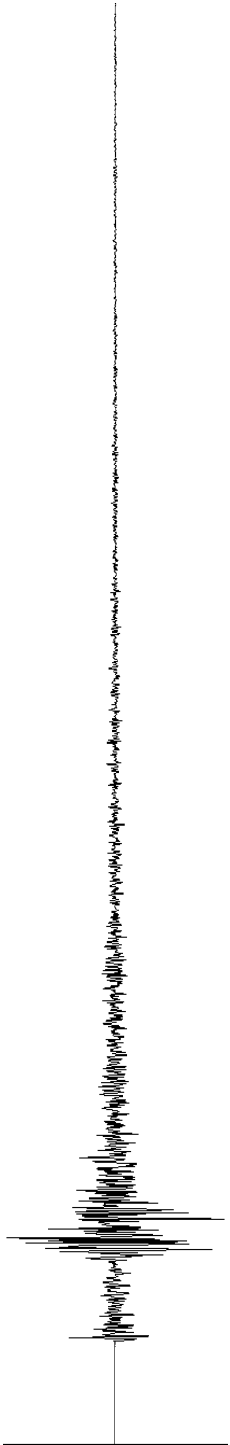
Inversion methods



Inversion methods



Need to apply **global search algorithms** to the non-linear multimodal problem!



Inversion methods

Simulated annealing

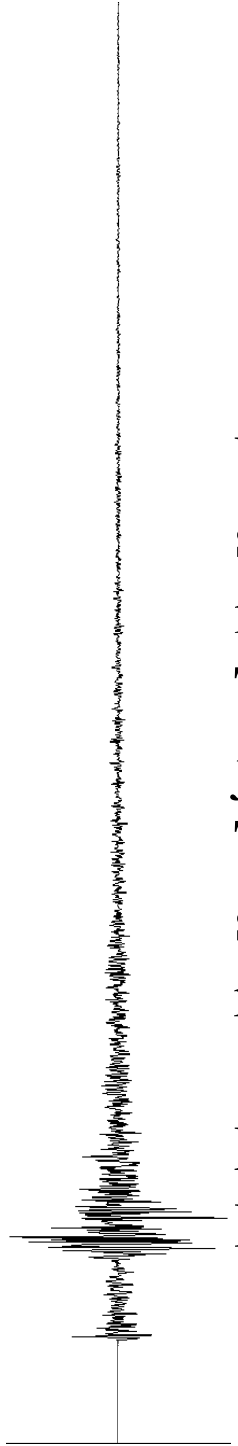
Uses an analogy with physical annealing in thermodynamic systems: for slowly cooling systems, nature is able to find minimum energy states.

Throughout the process the non-zero probability of long jumps allows the method to escape from local minima.

The method first searches widely (random walk) in model space (analog: high-temperature system), then the search is restricted and the algorithm freezes to the global minimum.

Metropolis et al., 1953: J. Chem. Phys., 21, 1087-1092.

Kirkpatrick et al., 1983: Science, 220, 671-680



Inversion methods

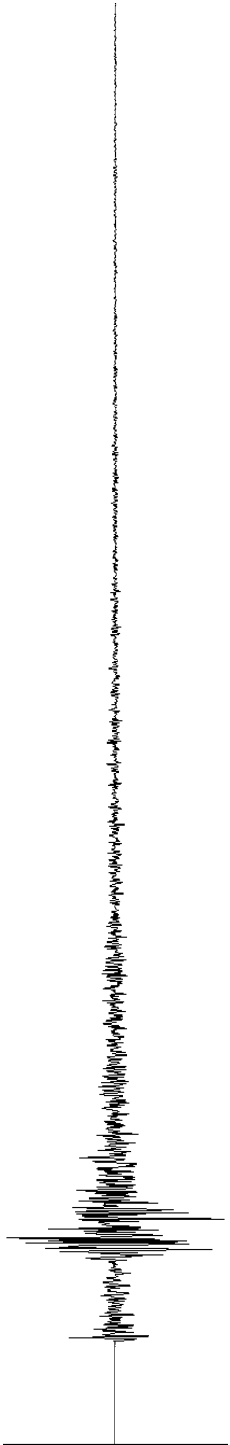
Hybrid global search algorithm

Simulated annealing algorithm initially searches widely to find an appropriate model that is not far from the global minimum, then the simplex algorithm moves to the global minimum itself.

Liu et al., 1995: JGR 122, 991-1000

Hartzell and Liu, 1995: BSSA 85, 516-524

Hartzell and Liu, 1996: PEPI, 95, 79-99 1992 Landers



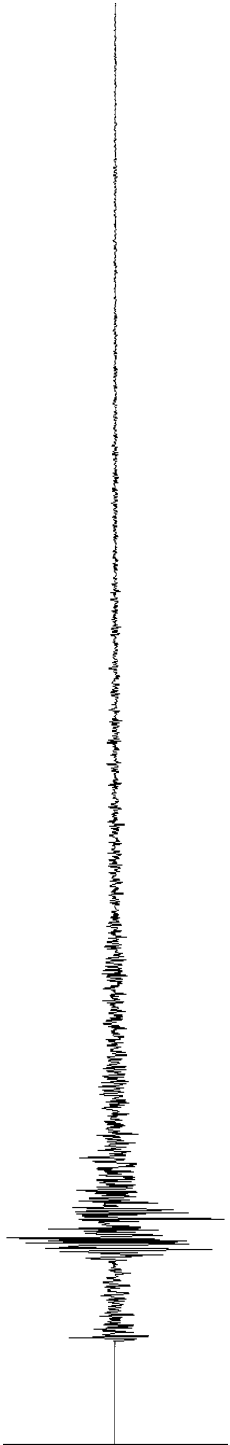
Inversion methods

Genetic algorithms

Based on analogies with the process of biological evolution
An initial population of models is selected at random and the GA seeks to improve the fitness of the population generation after generation. This is principally accomplished by the genetic processes of selection, crossover, and mutation.

Holland (1975) : *Adaptation in Natural and Artificial Systems*, Univ. Michigan Press.

Goldberg (1989): *Genetic Algorithms in Search, Optimization and Machine Learning*, Addison Wesley.



Inversion methods

Linear programming with L1 norm minimization

Used with only weak causality constraints on rupture times.
Can incorporate many physical constraints and thus stabilize the problem.

Das and Kostrov, 1990

1986 Andreanoff Isl.

Das and Kostrov, 1994

1989 Macquarie Ridge

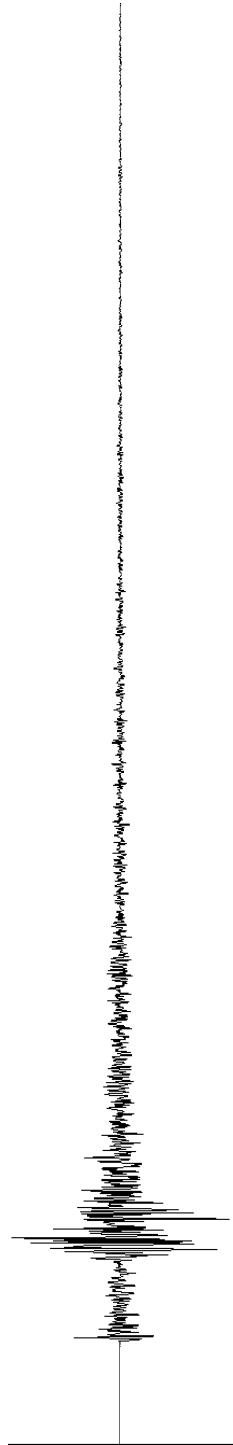
Das and Suhadolc, 1996

Synthetic cases - line source

Sarao' et al., 1998

Synthetic cases - planar source

Able to find global minimum, can apply time-domain constraints.



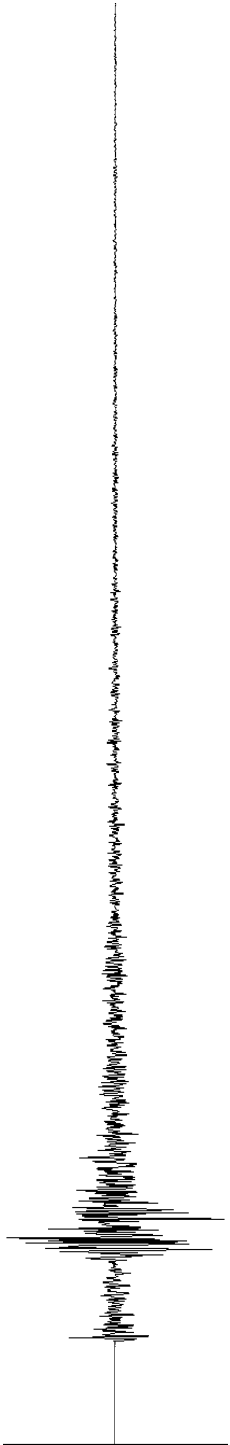
Forward and inverse problems

- ✓ Forward problem

$$\mathbf{d} = \mathbf{G} \mathbf{m}$$

- ✓ Inverse problem

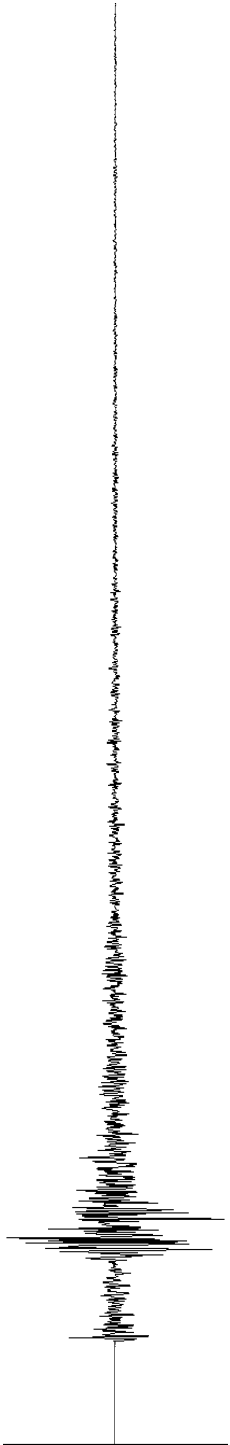
$$\mathbf{m}_p = \mathbf{G}_p^{-1} \mathbf{d}$$



Point- source case

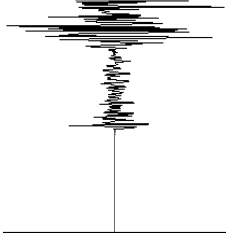
Two methods will be presented:

1. Inversion for a double-couple source
2. Inversion for a moment tensor



Method

Mao et al.,
1994



$$s_j = \phi_j(x_1, \dots, x_N)$$

seismogram model parameters

Minimize

$$\sum_j (o_j - s_j)^2 = \sum_j r_j^2 = \underline{r}^T \underline{r}$$

Linearizing one can show that the variations $\underline{\delta x}$ to the model parameters are linked to the misfit vector \underline{r} by

$$\underline{A} \underline{\delta x} = \underline{r}$$

with

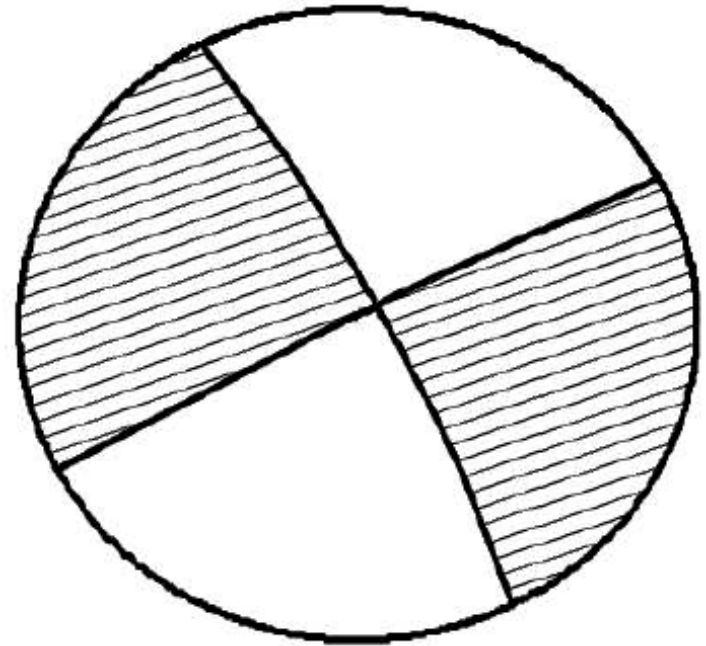
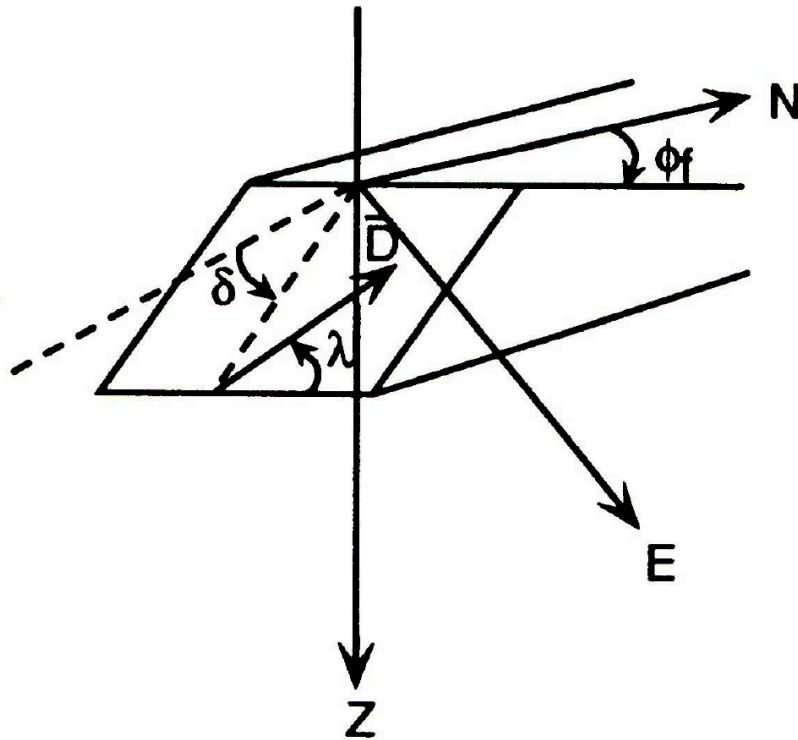
$$A_{ij} = \partial \phi_i / \partial x_j$$

To determine $\underline{\delta x}$ we use the SVD with a damping factor

$$\underline{\delta x} = \underline{A}^{-1} \underline{r} = \underline{A}^{\dagger} \underline{r} = \underline{V} (\underline{\Lambda}^2 + \theta^2 \underline{I})^{-1} \underline{\Lambda} \underline{U}^T \underline{r}$$

The value θ^2 varies at each step of the iteration process leading to the minimum.

Source mechanism: Fault and its representation



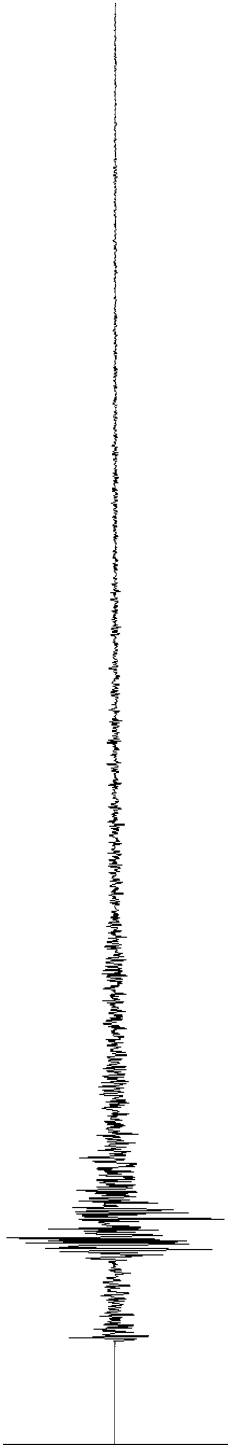
ϕ_f *strike*

δ *dip*

λ *rake*

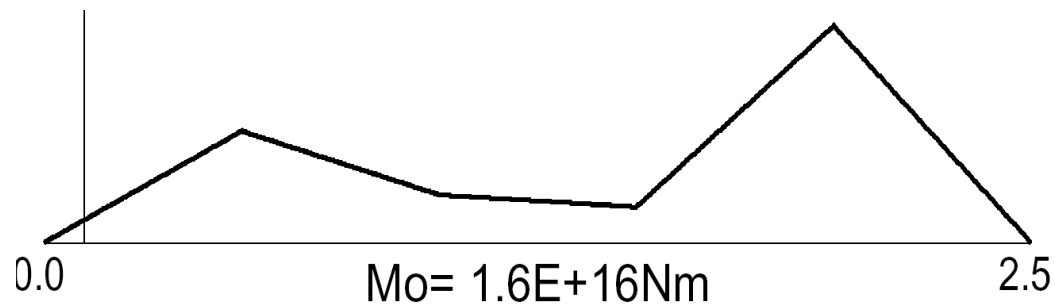
Lay, T. e Wallace, T. C. (1995). Modern global seismology, Academic Press.

ICTP 2004



Source time function and seismic moment

- ✓ $M_0 = \mu \hat{\mathbf{u}} \mathbf{S}$
- ✓ Seismic moment vs time
- ✓ Parametrized with triangles

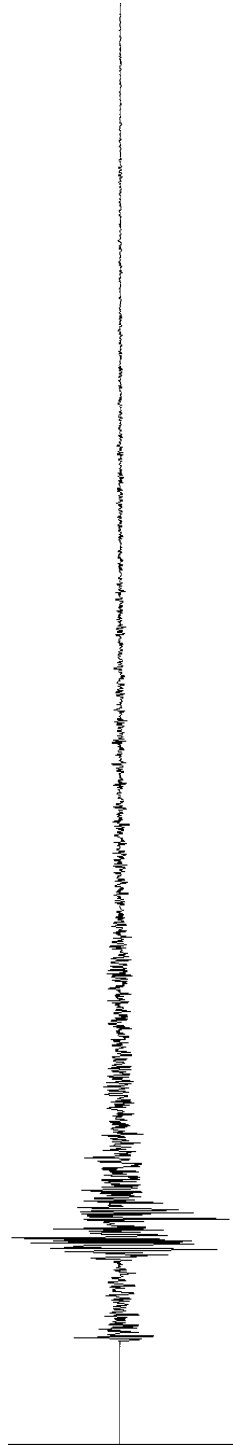


Linearized inversion: Taylor series expansion

- ✓ We approximate a seismogram as a function of its partial derivatives

$$s(p_1, \dots, p_m, t) = s(p_{10}, \dots, p_{m0}) + \frac{\partial}{\partial p_1} s(p_{10}, \dots, p_{m0}) \Delta p_1 + \dots \\ \dots + \frac{\partial}{\partial p_m} s(p_{10}, \dots, p_{m0}) \Delta p_m$$

and we consider its variations with respect to an initial seismogram



Formalism

- ✓ The inverse problem becomes

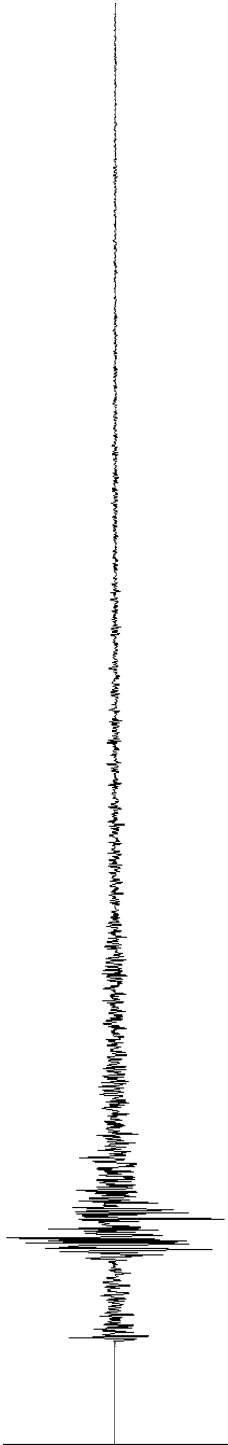
$$\mathbf{A}\delta\mathbf{x} = \mathbf{r}$$

\mathbf{A} partial derivatives matrix

$\delta\mathbf{x}$ parameters increment

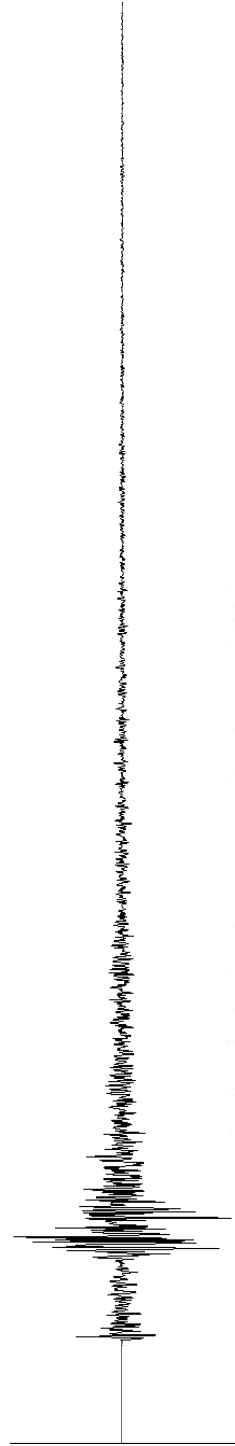
\mathbf{r} residuals

Mao, W. J., Panza, G. F. e Suhadolc, P. (1994) Linearized waveform inversion of local and near regional events for source mechanism and rupturing processes, *Geophys. J. Int* 116,784-798.



Matrix A

$$\begin{array}{cccccccc}
 \frac{\partial s_1(t_1)}{\partial \xi} & \frac{\partial s_1(t_1)}{\partial \eta} & \frac{\partial s_1(t_1)}{\partial \lambda} & \frac{\partial s_1(t_1)}{\partial h} & \frac{\partial s_1(t_1)}{\partial x} & \frac{\partial s_1(t_1)}{\partial y} & \frac{\partial s_1(t_1)}{\partial w_1} & \dots & \frac{\partial s_1(t_1)}{\partial w_K} \\
 \vdots & \vdots & \vdots & \vdots & \vdots & \vdots & \vdots & \dots & \vdots \\
 \frac{\partial s_1(t_{m1})}{\partial \xi} & \frac{\partial s_1(t_{m1})}{\partial \eta} & \frac{\partial s_1(t_{m1})}{\partial \lambda} & \frac{\partial s_1(t_{m1})}{\partial h} & \frac{\partial s_1(t_{m1})}{\partial x} & \frac{\partial s_1(t_{m1})}{\partial y} & \frac{\partial s_1(t_{m1})}{\partial w_1} & \dots & \frac{\partial s_1(t_{m1})}{\partial w_K} \\
 \dots & \dots & \dots & \dots & \dots & \dots & \dots & \dots & \dots \\
 \frac{\partial s_n(t_1)}{\partial \xi} & \frac{\partial s_n(t_1)}{\partial \eta} & \frac{\partial s_n(t_1)}{\partial \lambda} & \frac{\partial s_n(t_1)}{\partial h} & \frac{\partial s_n(t_1)}{\partial x} & \frac{\partial s_n(t_1)}{\partial y} & \frac{\partial s_n(t_1)}{\partial w_1} & \dots & \frac{\partial s_n(t_1)}{\partial w_K} \\
 \vdots & \vdots & \vdots & \vdots & \vdots & \vdots & \vdots & \dots & \vdots \\
 \frac{\partial s_n(t_{mn})}{\partial \xi} & \frac{\partial s_n(t_{mn})}{\partial \eta} & \frac{\partial s_n(t_{mn})}{\partial \lambda} & \frac{\partial s_n(t_{mn})}{\partial h} & \frac{\partial s_n(t_{mn})}{\partial x} & \frac{\partial s_n(t_{mn})}{\partial y} & \frac{\partial s_n(t_{mn})}{\partial w_1} & \dots & \frac{\partial s_n(t_{mn})}{\partial w_K}
 \end{array}$$



Singular values decomposition

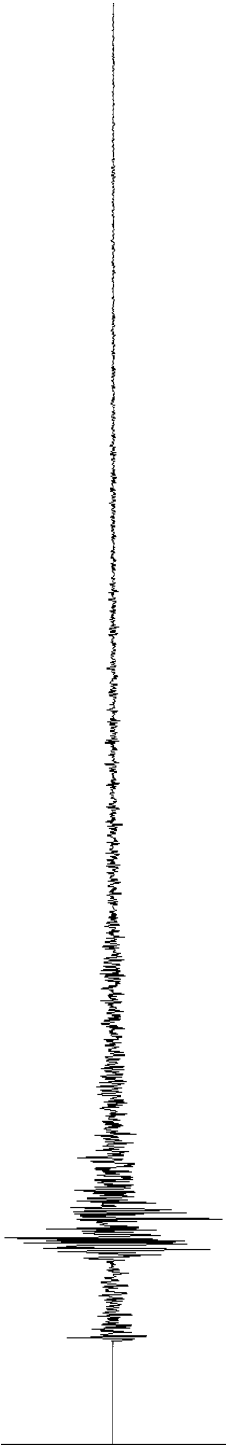
- Method to invert a rectangular matrix, expressing it in the form

$$\mathbf{A} = \mathbf{U}\mathbf{\Lambda}\mathbf{V}^T$$

$$\begin{bmatrix} 0 & \mathbf{A} \\ \mathbf{A}^T & 0 \end{bmatrix} \begin{bmatrix} \mathbf{u}_i \\ \mathbf{v}_i \end{bmatrix} = \lambda_i \begin{bmatrix} \mathbf{u}_i \\ \mathbf{v}_i \end{bmatrix}$$

– No unique solution

Menke, W. (1984). Geophysical data analysis: discrete inverse theory, Academic Press, Orlando.



Spectral component of seismogram mode summation method

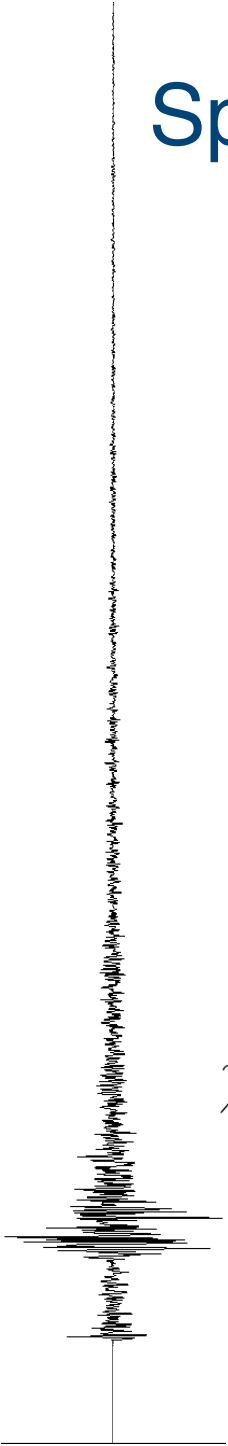
$$U = S k e^{-i3\pi/4} \chi(\theta, h) E \frac{e^{-ikr}}{r^{1/2}}$$

$$E_R = \epsilon_0 A_R k_r^{-1/2}$$

$$E_L = A_L k_L^{-1/2}$$

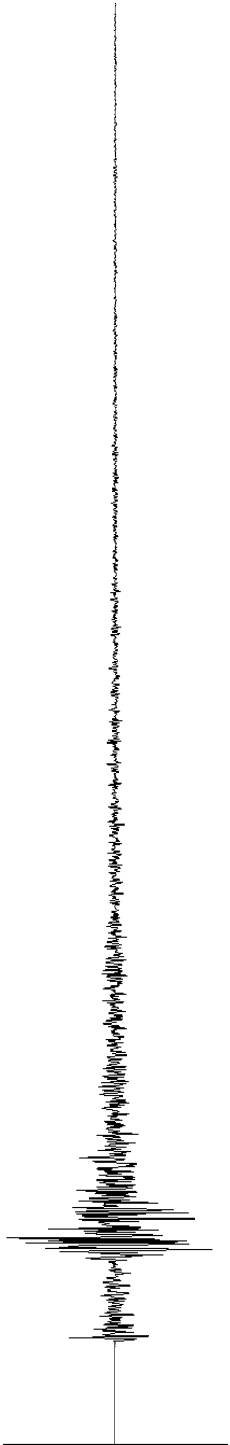
$$\chi = d_0 + i(d_1 \sin \theta + d_2 \cos \theta) + d_3 \sin 2\theta + d_4 \cos 2\theta$$

Harkrider, 1970; Panza, 1985.



Radiation pattern coefficients

coefficiente	Love	Rayleigh
d_0	0	$\frac{1}{2} \sin \lambda \sin 2\delta B(h)$
d_1	$\cos \lambda \cos \delta G(h)$	$-\sin \lambda \cos 2\delta C(h)$
d_2	$-\sin \lambda \cos 2\delta G(h)$	$-\cos \lambda \cos \delta C(h)$
d_3	$\frac{1}{2} \sin \lambda \cos 2\delta V(h)$	$\cos \lambda \sin \delta A(h)$
d_4	$\cos \lambda \sin \delta V(h)$	$-\frac{1}{2} \sin \lambda \sin 2\delta A(h)$



Eigenfunctions: stresses and velocities

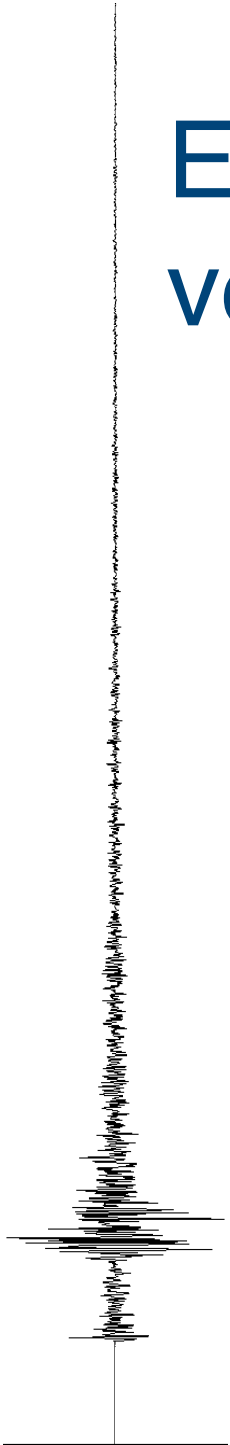
$$A(h) = -\frac{\dot{u}_s^*(h)}{\dot{w}_0}$$

$$B(h) = -\left(3 - 4\frac{\beta_s^2}{\alpha_s^2}\right) \frac{\dot{u}_s^*(h)}{\dot{w}_0} - \frac{2}{\rho_s \alpha_s^2} \frac{\sigma_{Rs}^*(h)}{\frac{\dot{w}_0}{c_R}}$$

$$C(h) = -\frac{1}{\mu_S} \left[\frac{\tau_{Rs}(h)}{\frac{\dot{w}_0}{c_R}} \right]$$

$$G(h) = \frac{1}{\mu_S} \left[\frac{\tau_{Ls}^*(h)}{\frac{\dot{v}_0}{c_L}} \right]$$

$$V(h) = \frac{\dot{v}_s(h)}{\dot{v}_0}$$



Analytical differentiation: angles

v Rayleigh

– Strike

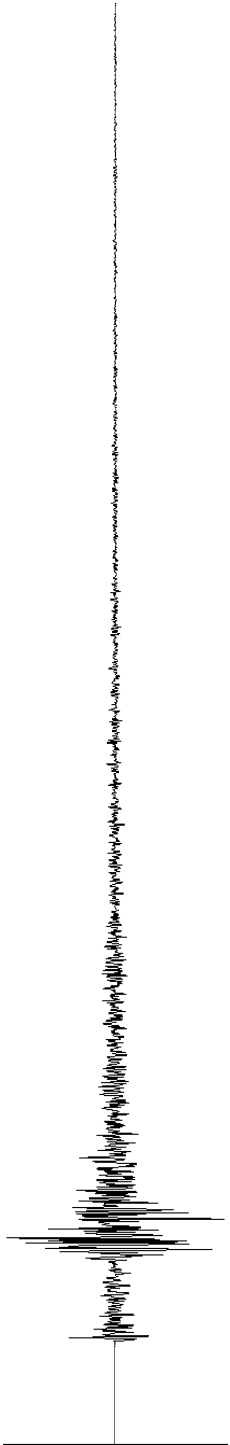
$$\begin{aligned}\frac{\partial \chi}{\partial \theta} = & i(-\cos \theta \sin \lambda \cos 2\delta C(h) + \sin \theta \cos \lambda \cos \delta C(h)) \\ & + 2 \cos 2\theta \cos \lambda \sin \delta A(h) + \sin 2\theta \sin \lambda \sin 2\delta A(h)\end{aligned}$$

– Dip

$$\begin{aligned}\frac{\partial \chi}{\partial \delta} = & \sin \lambda \cos 2\delta B(h) + i(2 \sin \theta \sin \lambda \sin 2\delta C(h) + \cos \theta \cos \lambda \sin \delta C(h)) \\ & + \sin 2\theta \cos \lambda \cos \delta A(h) - \cos 2\theta \sin \lambda \cos 2\delta A(h) \quad (2.\end{aligned}$$

– Rake

$$\begin{aligned}\frac{\partial \chi}{\partial \lambda} = & \frac{1}{2} \cos \lambda \sin 2\delta B(h) \\ & + i(-\sin \theta \cos \lambda \cos 2\delta C(h) + \cos \theta \sin \lambda \cos \delta C(h)) \\ & - \sin 2\theta \sin \lambda \sin \delta A(h) - \frac{1}{2} \cos 2\theta \cos \lambda \sin 2\delta A(h)\end{aligned}$$



Analytical differentiation: angles

v Love

– Strike

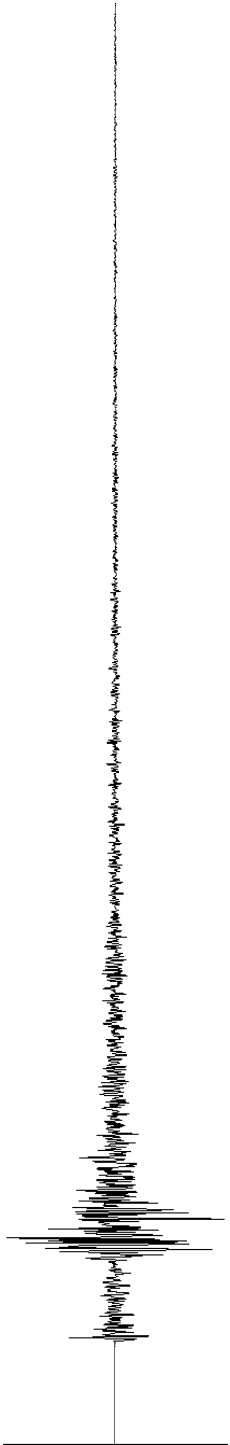
$$\begin{aligned}\frac{\partial \chi}{\partial \theta} = & i(\cos \theta \cos \lambda \cos \delta G(h) + \sin \theta \sin \lambda \cos 2\delta G(h)) \\ & + \cos 2\theta \sin \lambda \cos 2\delta V(h) - \sin 2\theta \cos \lambda \sin \delta V(h)\end{aligned}$$

– Dip

$$\begin{aligned}\frac{\partial \chi}{\partial \delta} = & -i(\sin \theta \cos \lambda \sin \delta G(h) - 2 \cos \theta \sin \lambda \sin 2\delta G(h)) \\ & - \sin 2\theta \sin \lambda \sin 2\delta V(h) - \cos 2\theta \cos \lambda \cos \delta V(h)\end{aligned}$$

– Rake

$$\begin{aligned}\frac{\partial \chi}{\partial \lambda} = & -i(\sin \theta \sin \lambda \cos \delta G(h) + \cos \theta \cos \lambda \cos 2\delta G(h)) \\ & + \frac{1}{2} \sin 2\theta \cos \lambda \cos 2\delta V(h) - \cos 2\theta \sin \lambda \sin \delta V(h)\end{aligned}$$



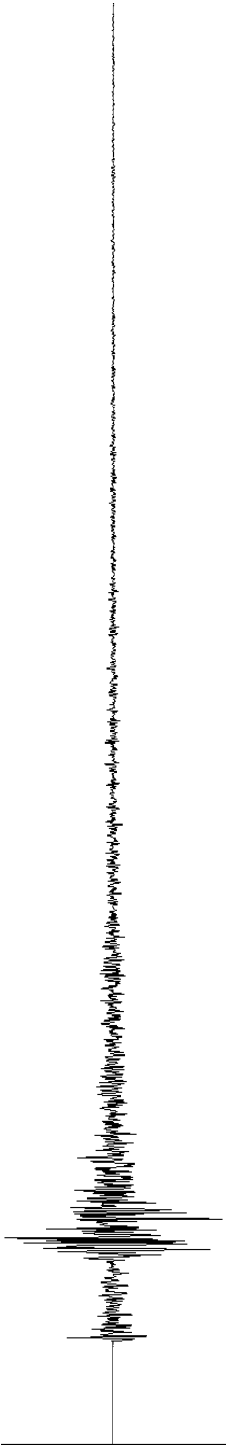
Analytical differentiation: distance

- Rayleigh and Love

$$\frac{\partial U}{\partial r} = \left(-ik + \frac{1}{2r} \right) S k^m e^{-i(1+2m)\pi/4} \chi(\theta, h) E \frac{e^{-ikr}}{r^{1/2}}$$

- From attenuation factors

$$e^{-\omega r C}$$



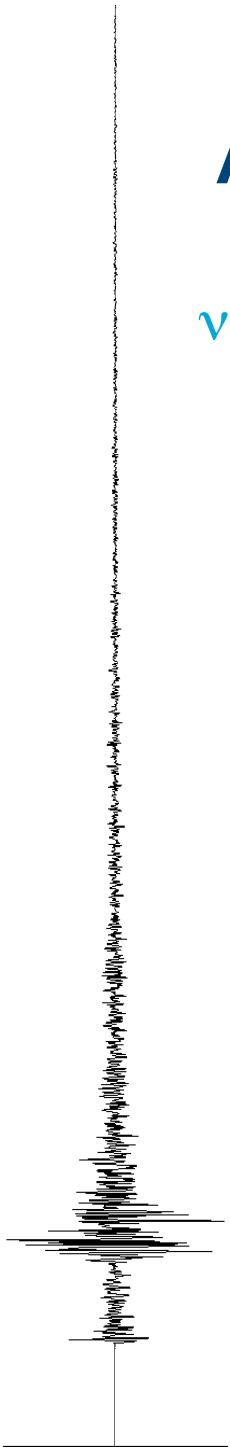
Analytical differentiation: depth

✓ Rayleigh

$$\frac{\partial A(h)}{\partial h} = \frac{\partial}{\partial h} \left[-\frac{\dot{u}^*(h)}{\dot{w}_0} \right] = k_R \left\{ \left[\frac{\dot{w}_s(h)}{\dot{w}_0} \right] + \frac{1}{\mu_s} \left[\frac{\tau_{Rs}(h)}{\frac{\dot{w}_0}{c_R}} \right] \right\}$$

$$\begin{aligned} \frac{\partial B(h)}{\partial h} &= -\frac{\partial}{\partial h} \left[\left(3 - 4 \frac{\beta_s^2}{\alpha_s^2} \right) \frac{\dot{u}_s^*(h)}{\dot{w}_0} + \frac{2}{\rho_s \alpha_s^2} \frac{\sigma_{Rs}^*(h)}{\frac{\dot{w}_0}{c_R}} \right] \\ &= - \left[\left(3 - 4 \frac{\beta_s^2}{\alpha_s^2} \right) k_R \left[\frac{\dot{w}_s(h)}{\dot{w}_0} + \frac{1}{\mu_s} \frac{\tau_{Rs}(h)}{\frac{\dot{w}_0}{c_R}} \right] \right] + \\ &\quad \frac{2}{\rho_s \alpha_s^2} k_R \left\{ \rho_s c_R^2 \left[\frac{\dot{w}_s(h)}{\dot{w}_0} \right] + \left[\frac{\tau_{Rs}(h)}{\frac{\dot{w}_0}{c_R}} \right] \right\} \end{aligned}$$

$$\begin{aligned} \frac{\partial C(h)}{\partial h} &= -\frac{\partial}{\partial h} \left\{ \frac{1}{\mu_s} \left[\frac{\tau_{Rs}(h)}{\frac{\dot{w}_0}{c_R}} \right] \right\} \\ &= -\frac{k_r}{\mu_s} \left\{ \frac{\lambda_s}{(\lambda_s + 2\mu_s)} \left[\frac{\sigma_{Rs}^*(h)}{\frac{\dot{w}_0}{c_R}} \right] + \left[\rho_s c_R^2 - \frac{4\mu_s(\lambda_s + \mu_s)}{(\lambda_s + 2\mu_s)} \right] \left[\frac{\dot{u}_s^*(h)}{\dot{w}_0} \right] \right\} \end{aligned}$$



Analytical differentiation: depth

v Love

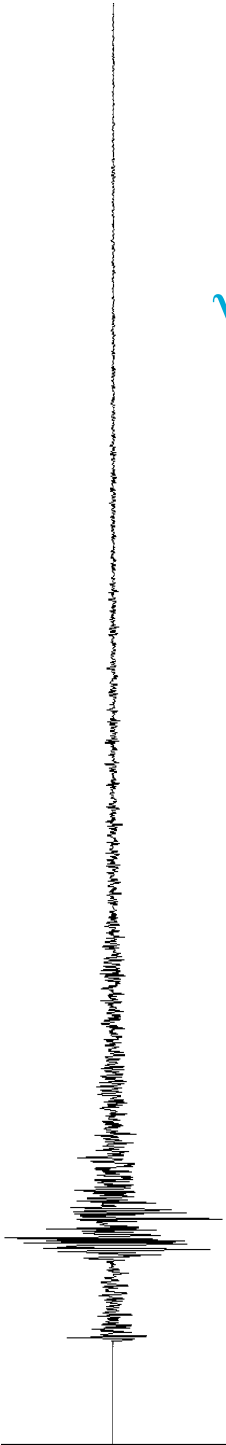
$$\frac{\partial G(h)}{\partial h} = -\frac{\partial}{\partial h} \left\{ \frac{1}{\mu_s} \left[\frac{\tau_r s^*(h)}{\frac{\dot{v}_0}{c_L}} \right] \right\} = \frac{k_L}{\mu_s} (\rho_s C_L^2 - \mu_s) \left[\frac{\dot{v}_s^*(h)}{\dot{v}_0} \right]$$

$$\frac{\partial V(h)}{\partial h} = \frac{\partial}{\partial h} \left[\frac{\dot{v}_s(h)}{\dot{v}_0} \right] = -\frac{k_L}{\mu_s} \left[\frac{\tau_L s^*(h)}{\frac{\dot{v}_0}{c_L}} \right]$$

that is

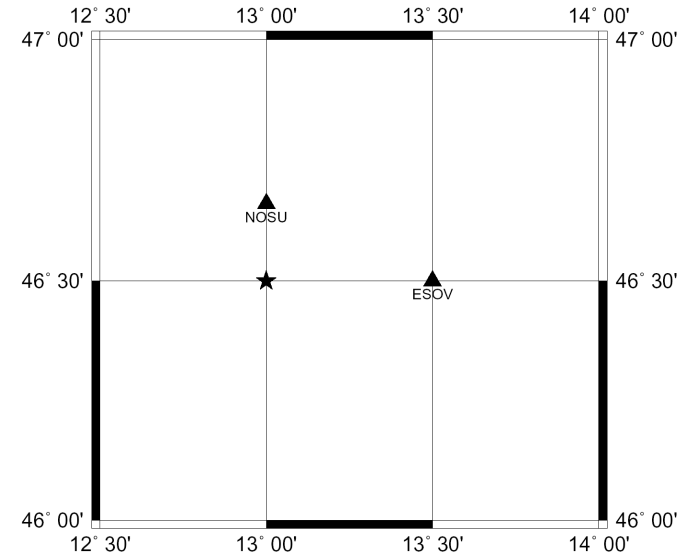
$$\frac{\partial G(h)}{\partial h} = \frac{k_L}{\mu_s} (\rho_s C_L^2 - \mu_s) V(h)$$

$$\frac{\partial V(h)}{\partial h} = -k_L G(h)$$

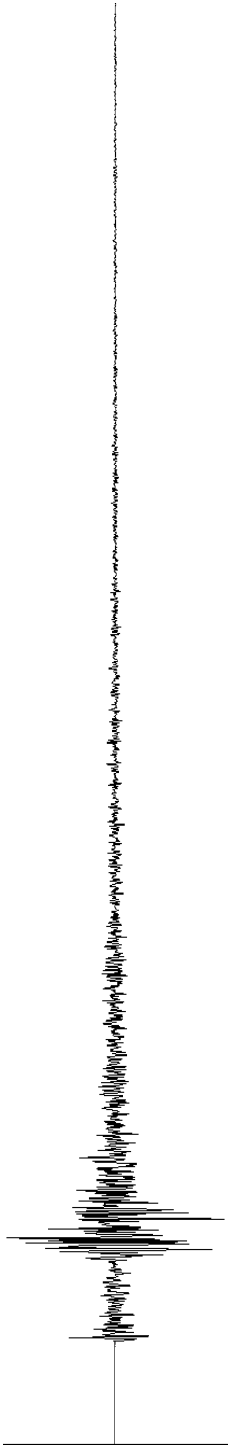
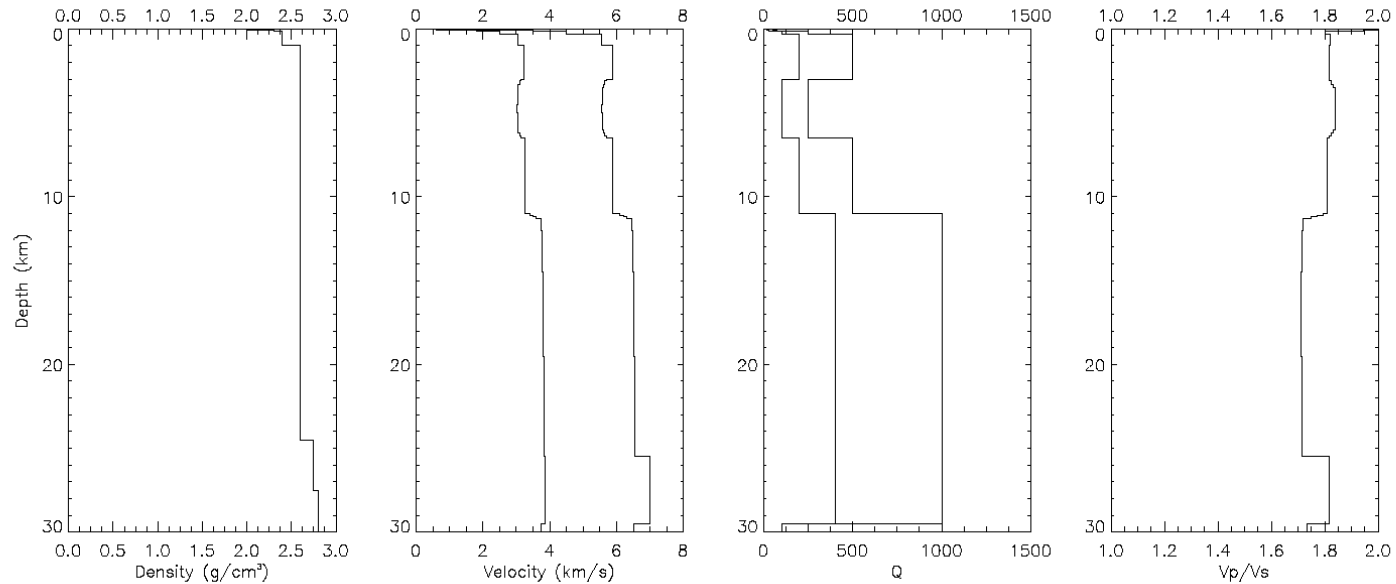


Synthetic test

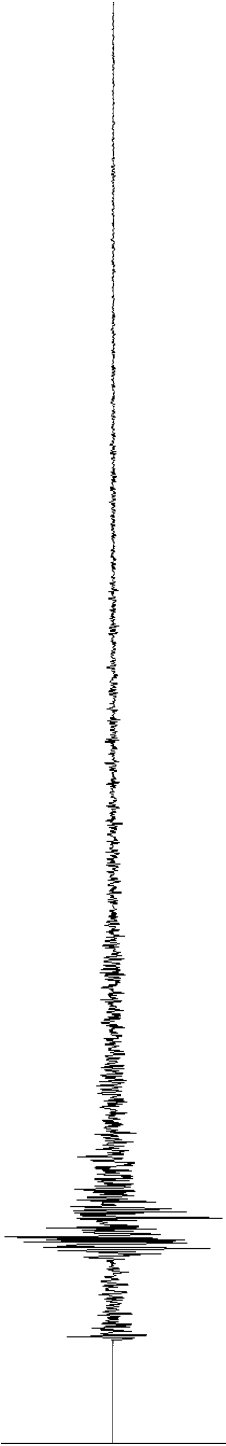
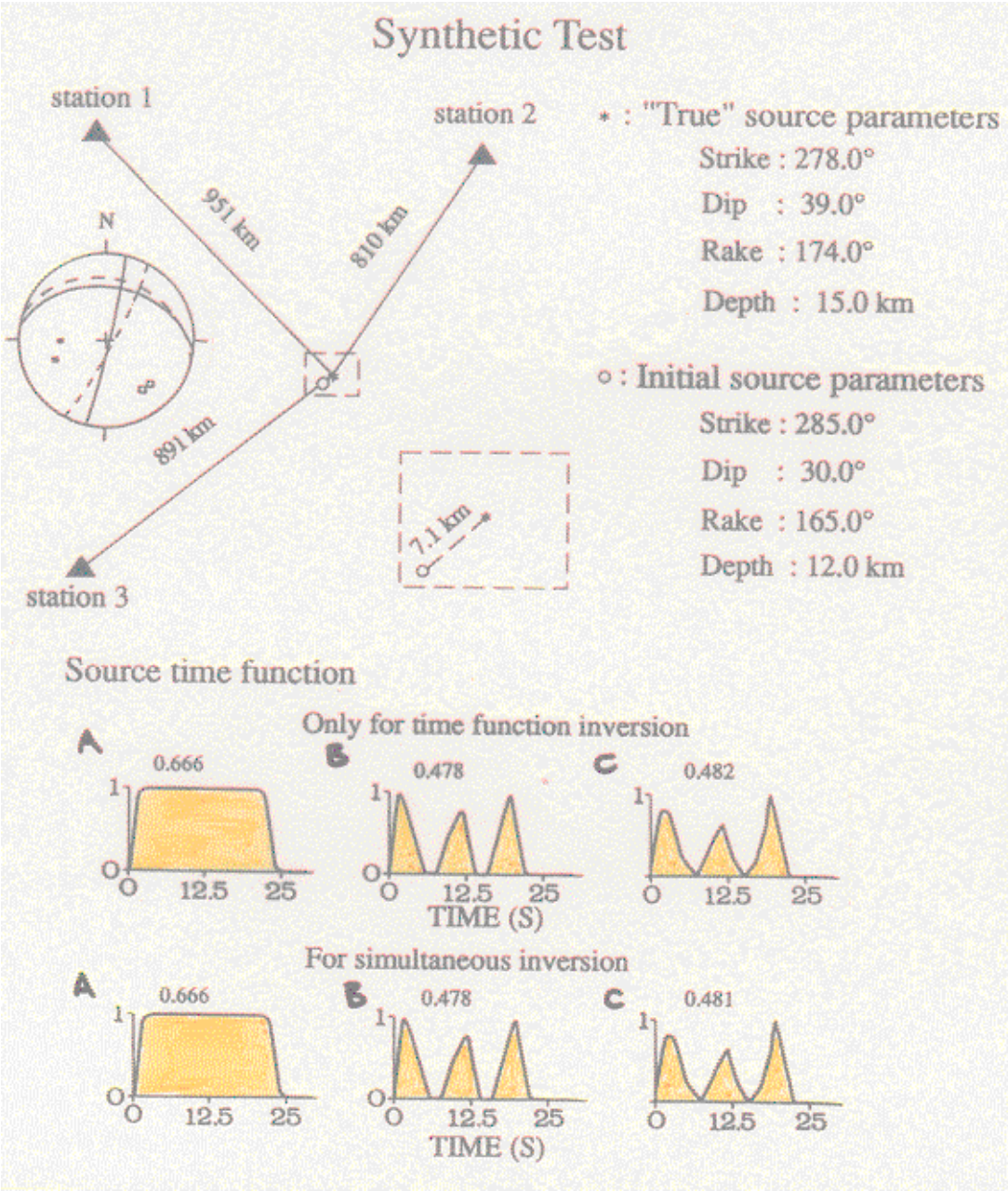
- ✓ Strike 120°
- ✓ Dip 80°
- ✓ Rake 10°



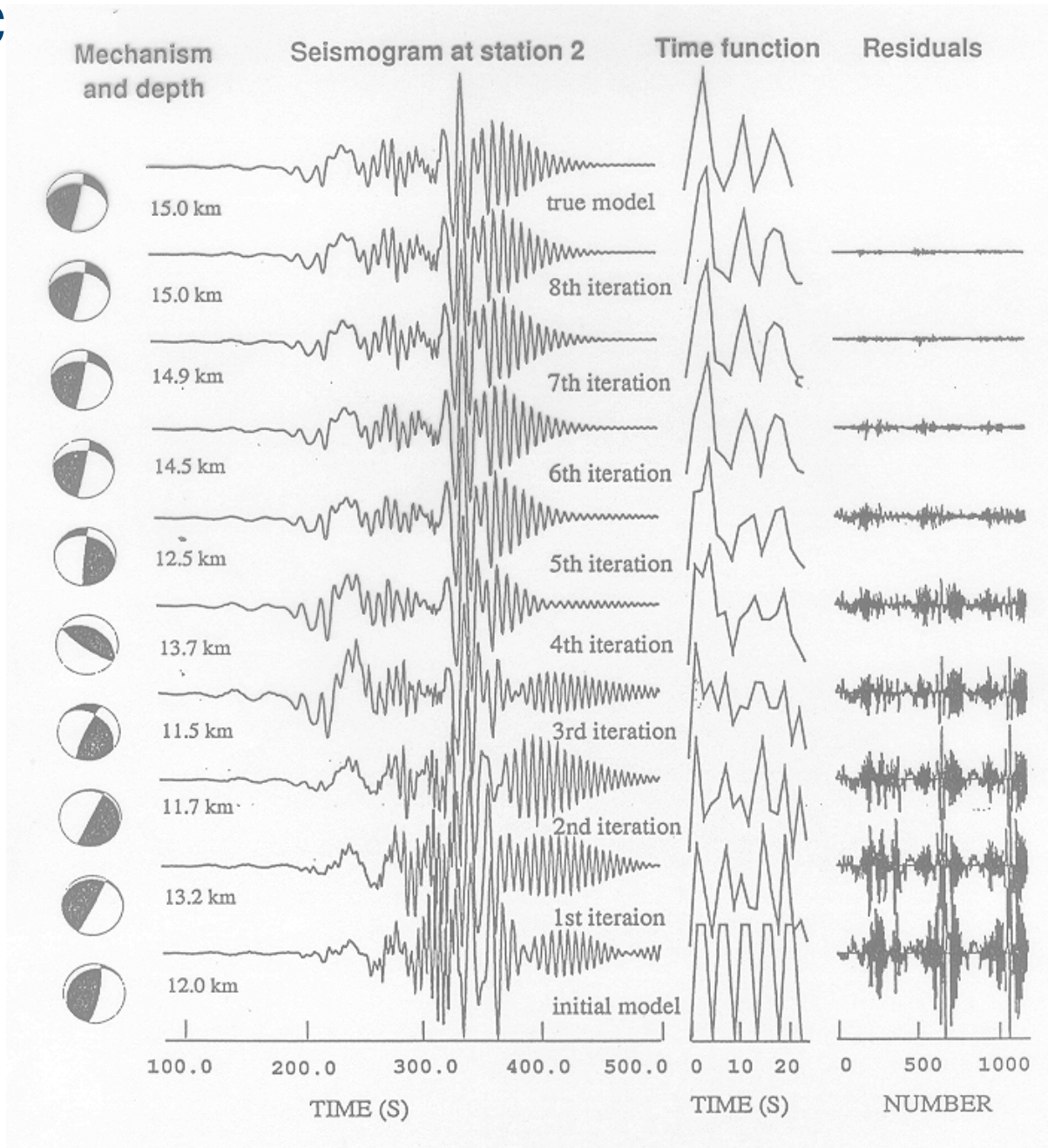
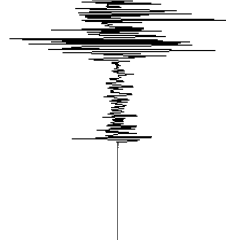
friul7w.str



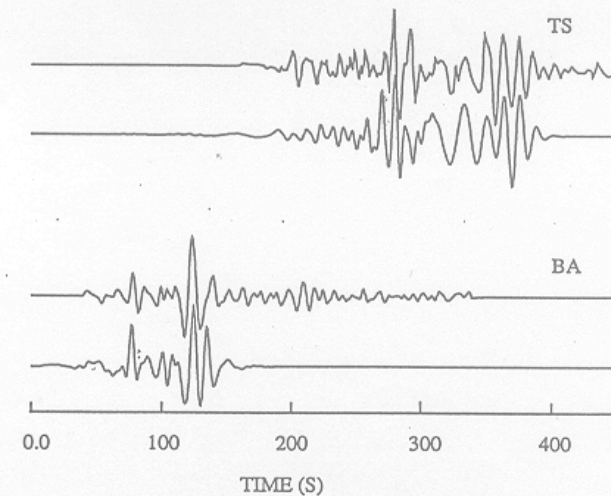
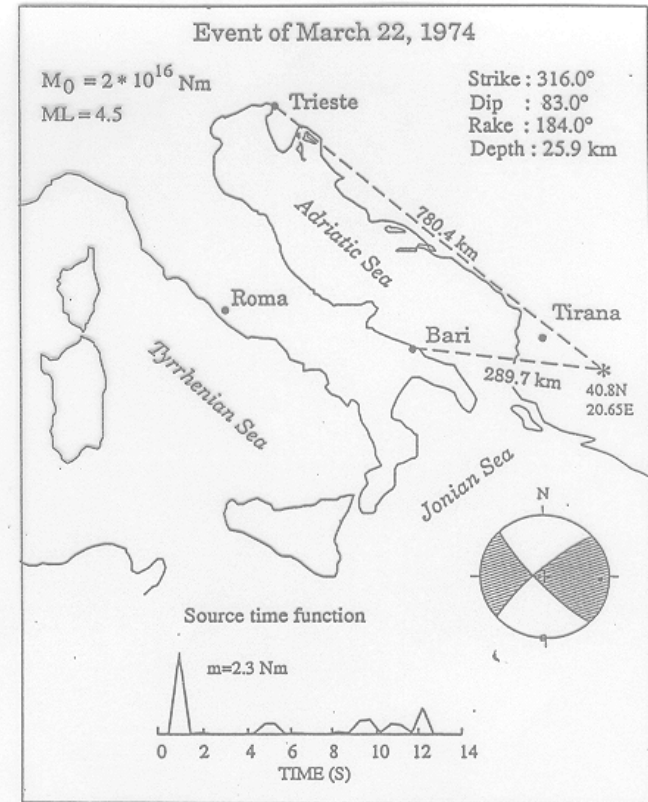
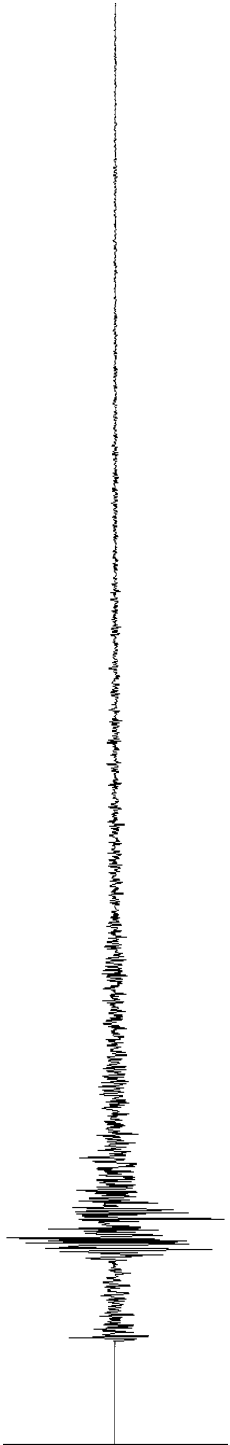
Slide



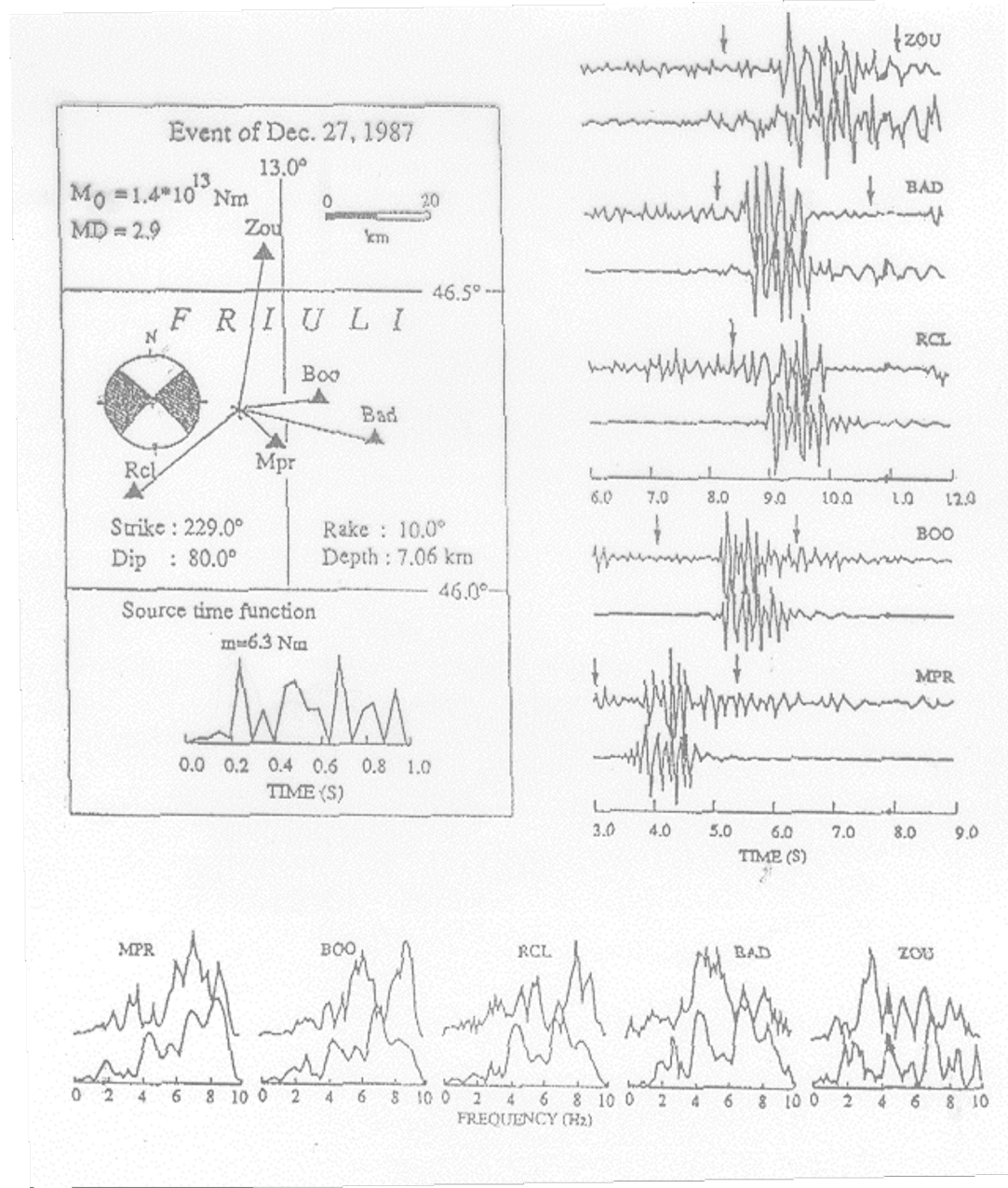
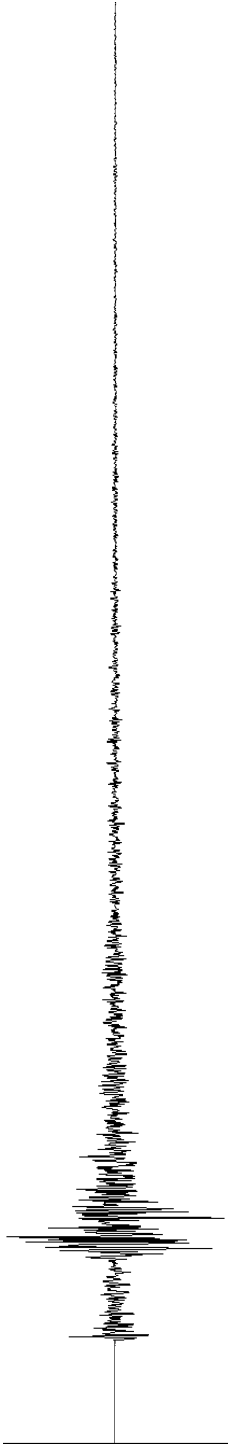
Convergence



Application to a regional event



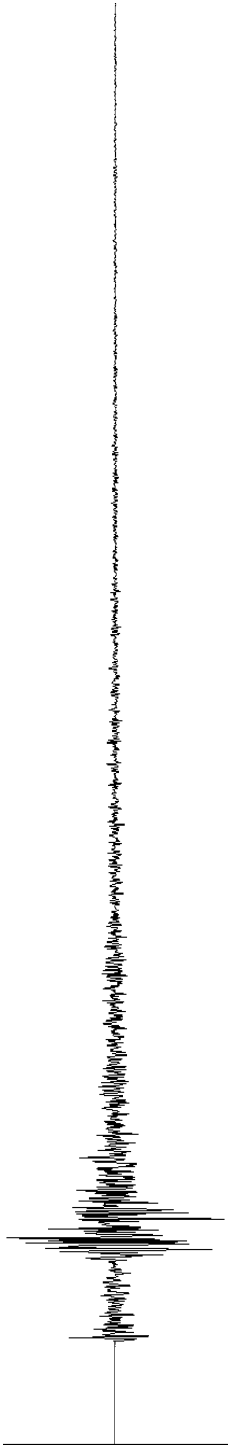
Local event



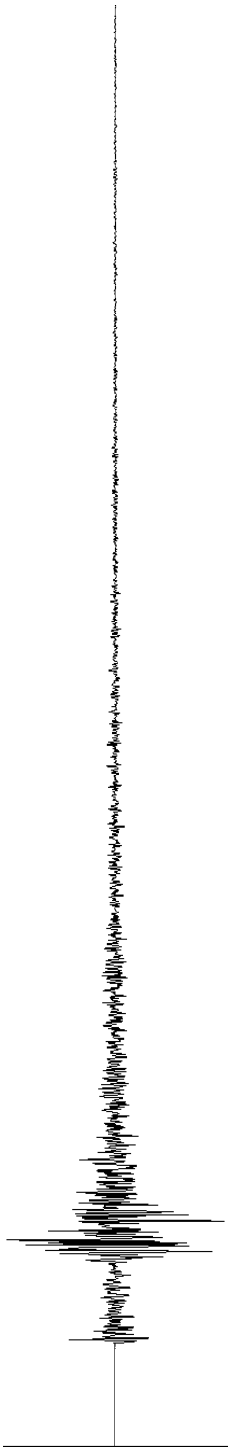
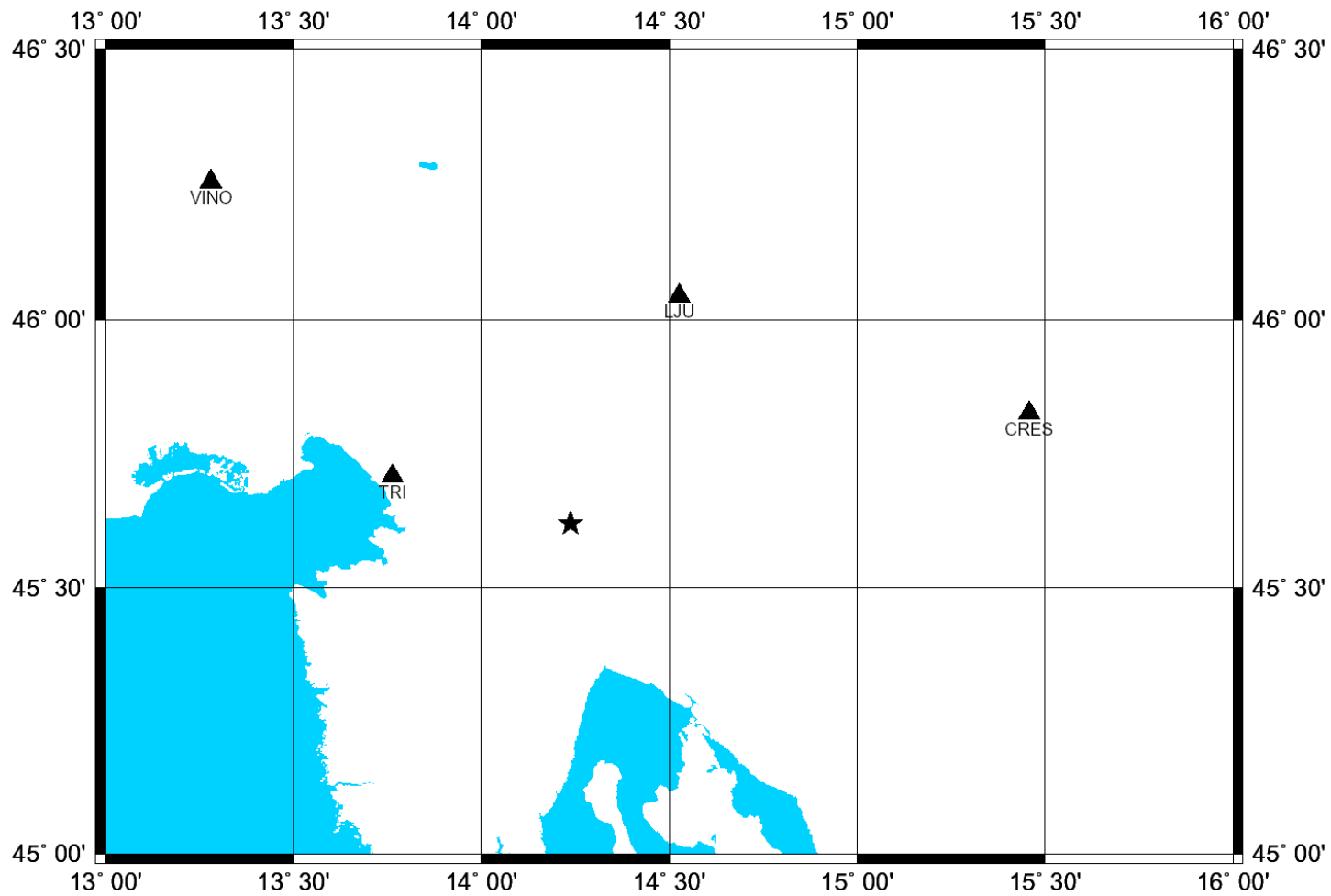
The event of June 2, 2002

v MI 3.8 (LJU)

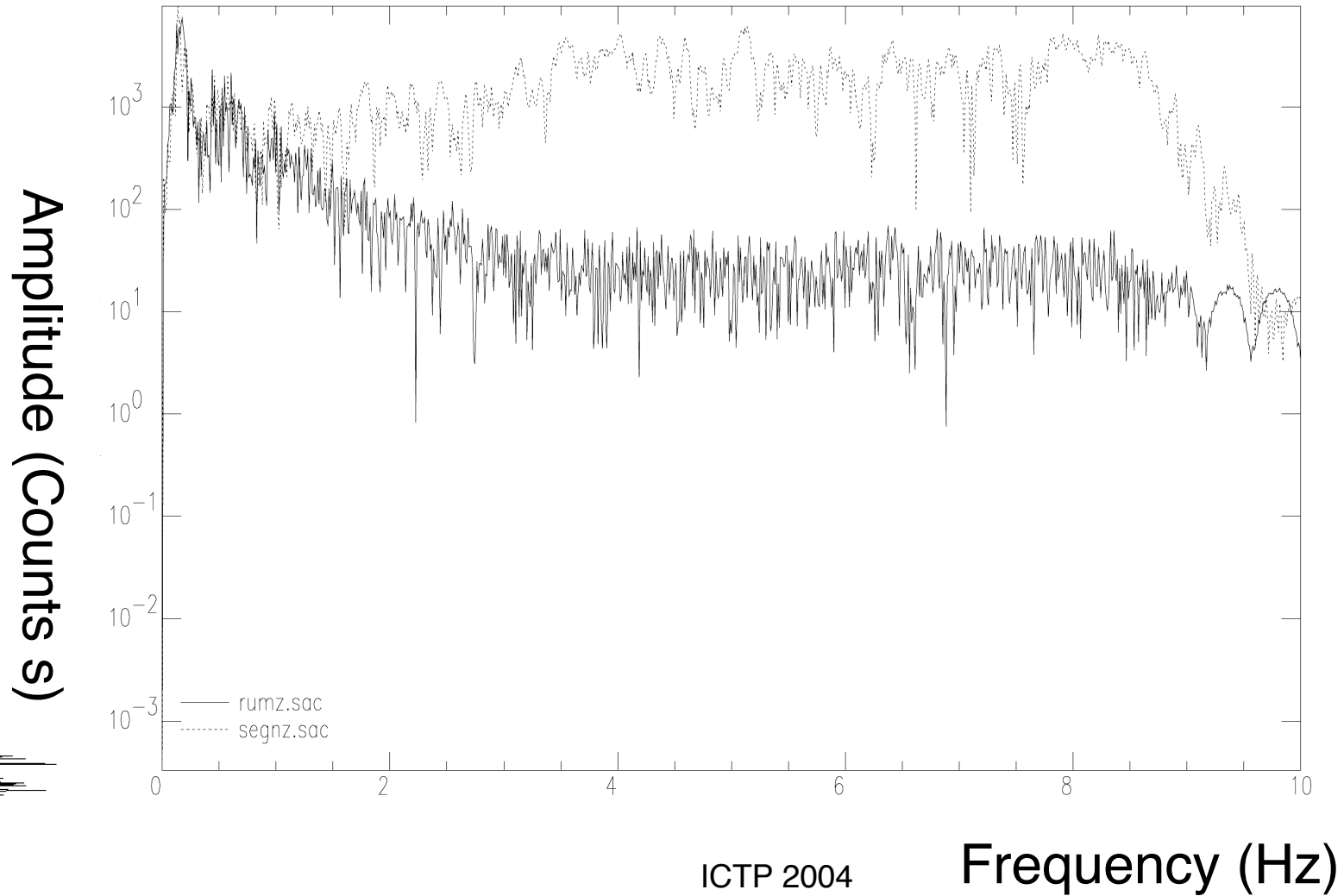
45.640° N 14.240° E



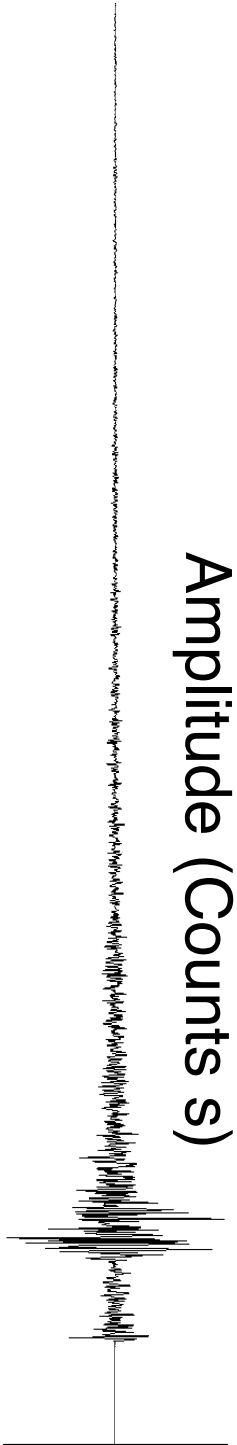
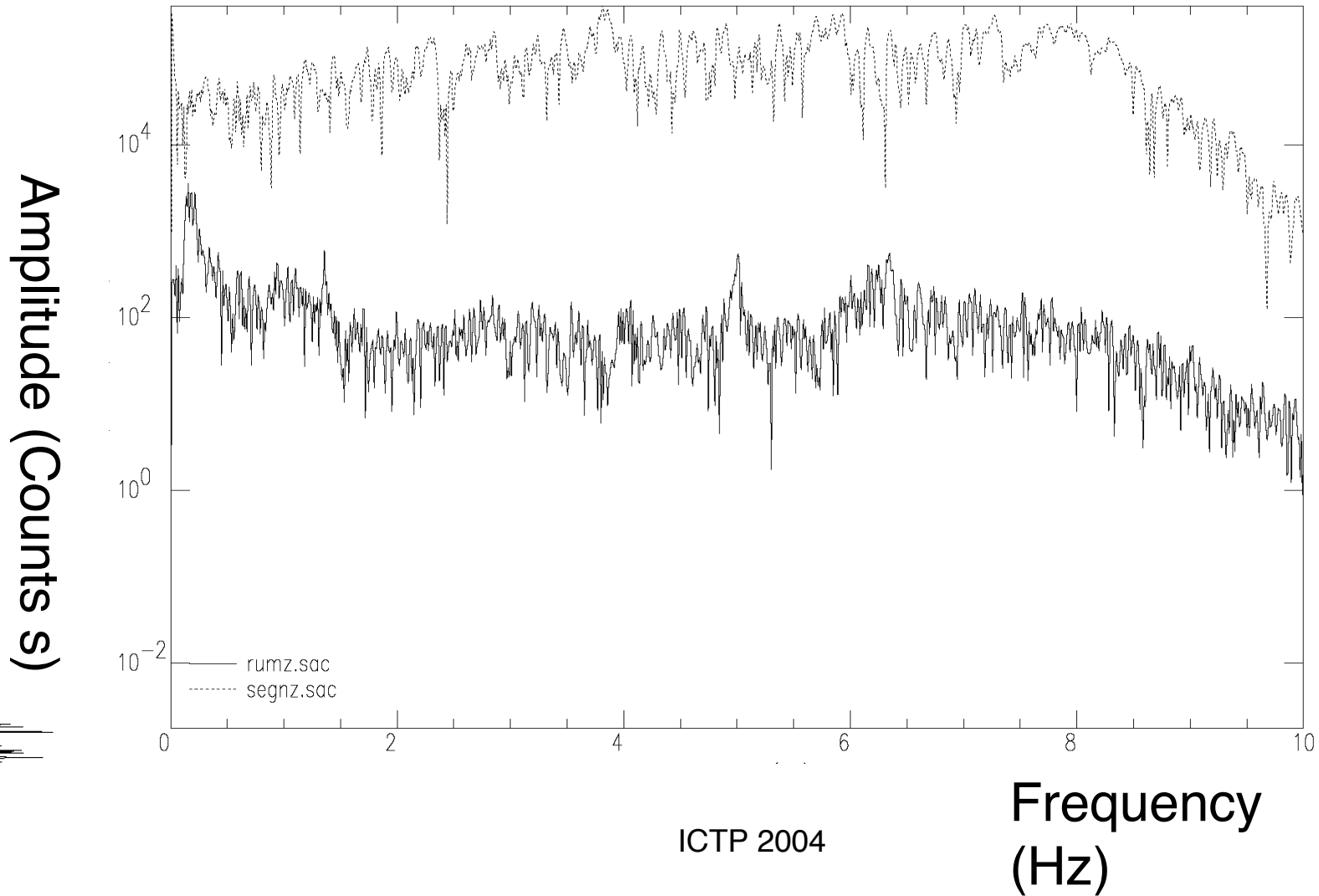
Stations used



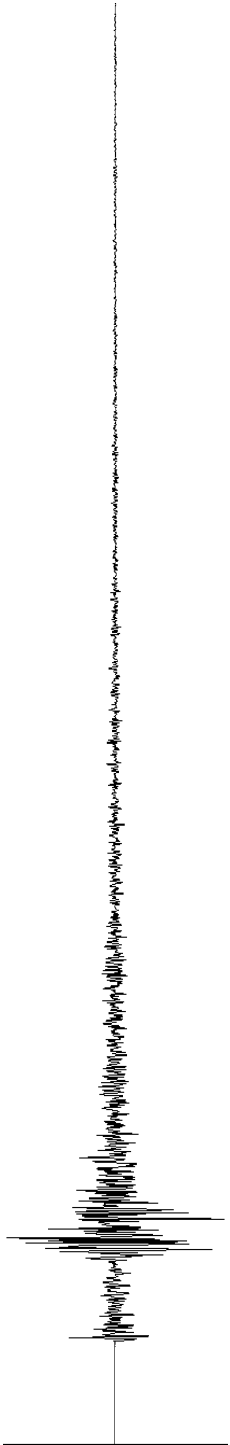
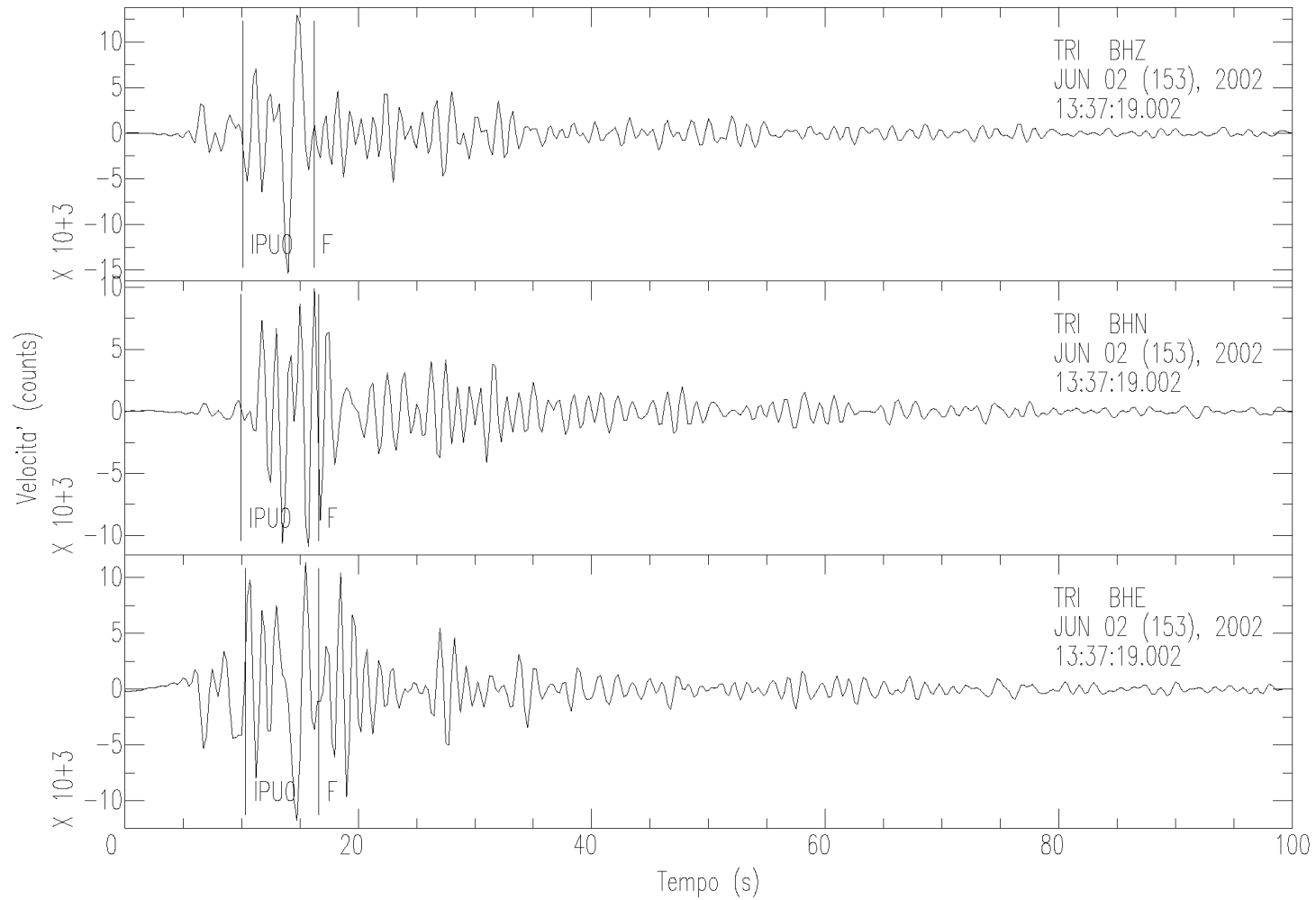
Noise vs signal spectra



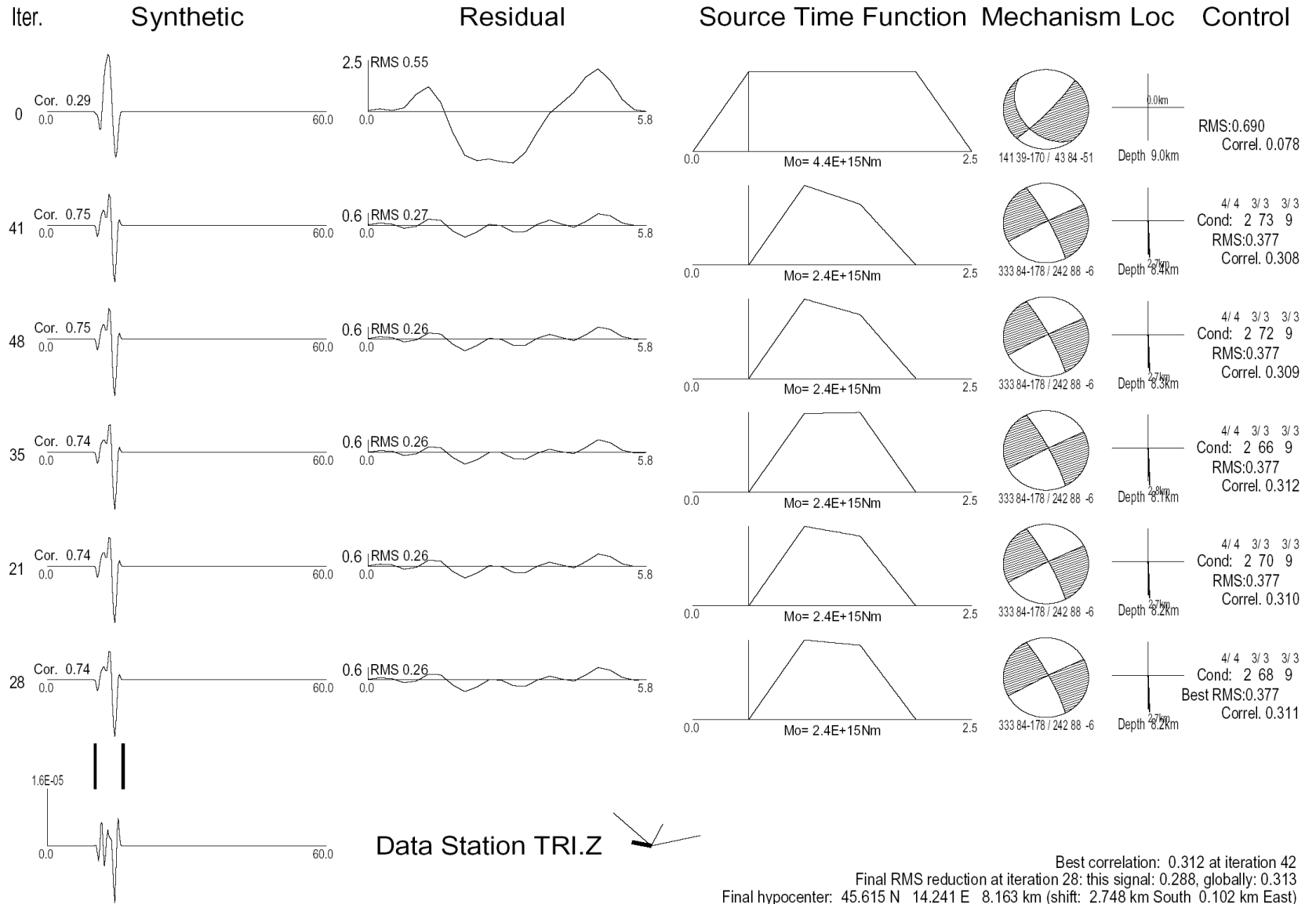
Noise vs signal spectra



Time windows for inversion



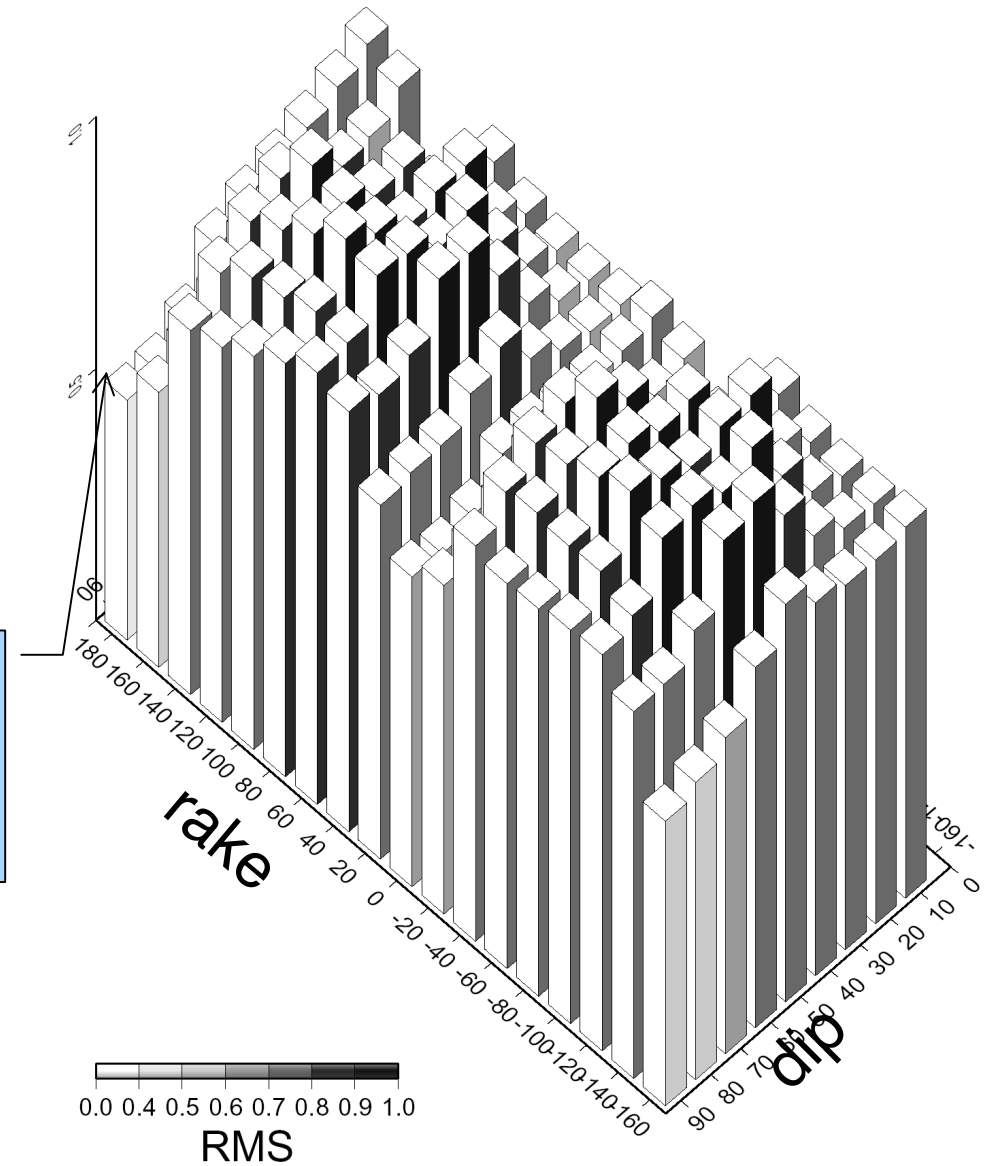
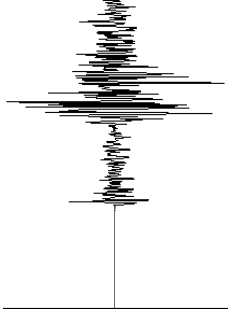
Results



Best correlation: 0.312 at iteration 42
 Final RMS reduction at iteration 28: this signal: 0.288, globally: 0.313
 Final hypocenter: 45.615 N 14.241 E 8.163 km (shift: 2.748 km South 0.102 km East)

Parameters space exploration

It is the same
minimum of the
inversion



seismo.ethz.ch

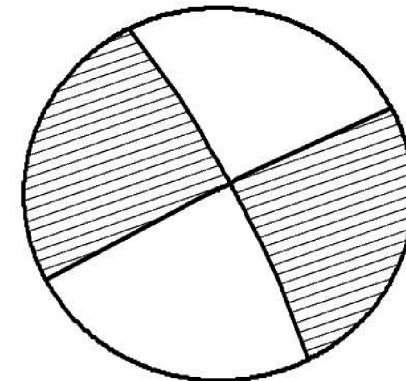
Best Fitting Double-Couple:

$M_0 = 7.89E+21$ dyn cm $M_w = 3.90$

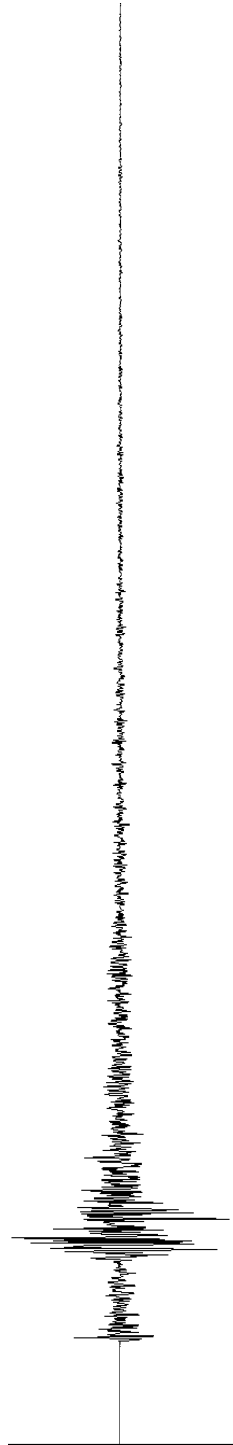
Plane Strike Rake Dip

NP1 66 16 79

NP2 333 168 74



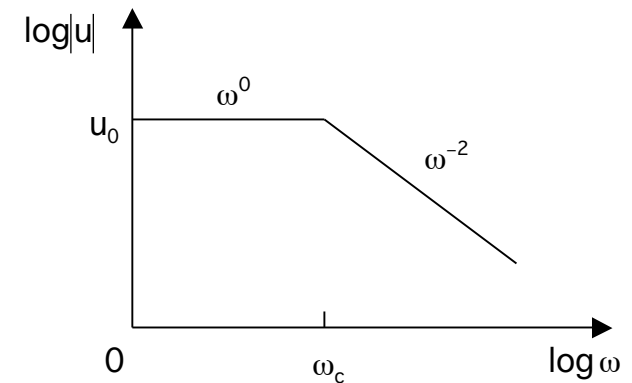
333 84-178 / 242 88 -6



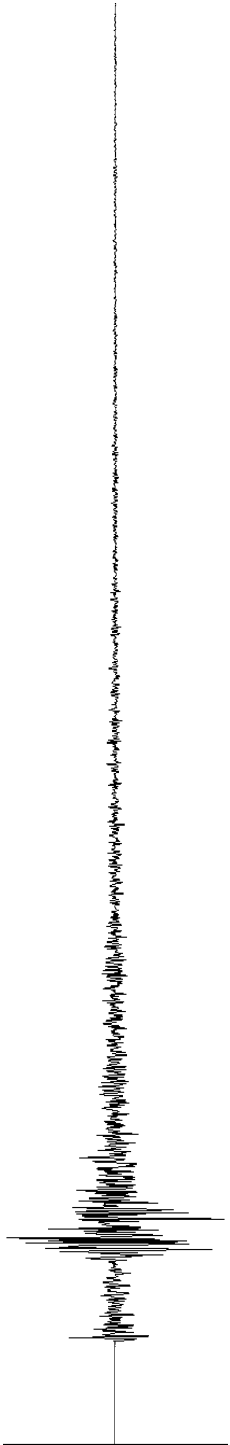
Seismic moment estimate

✓ We know:

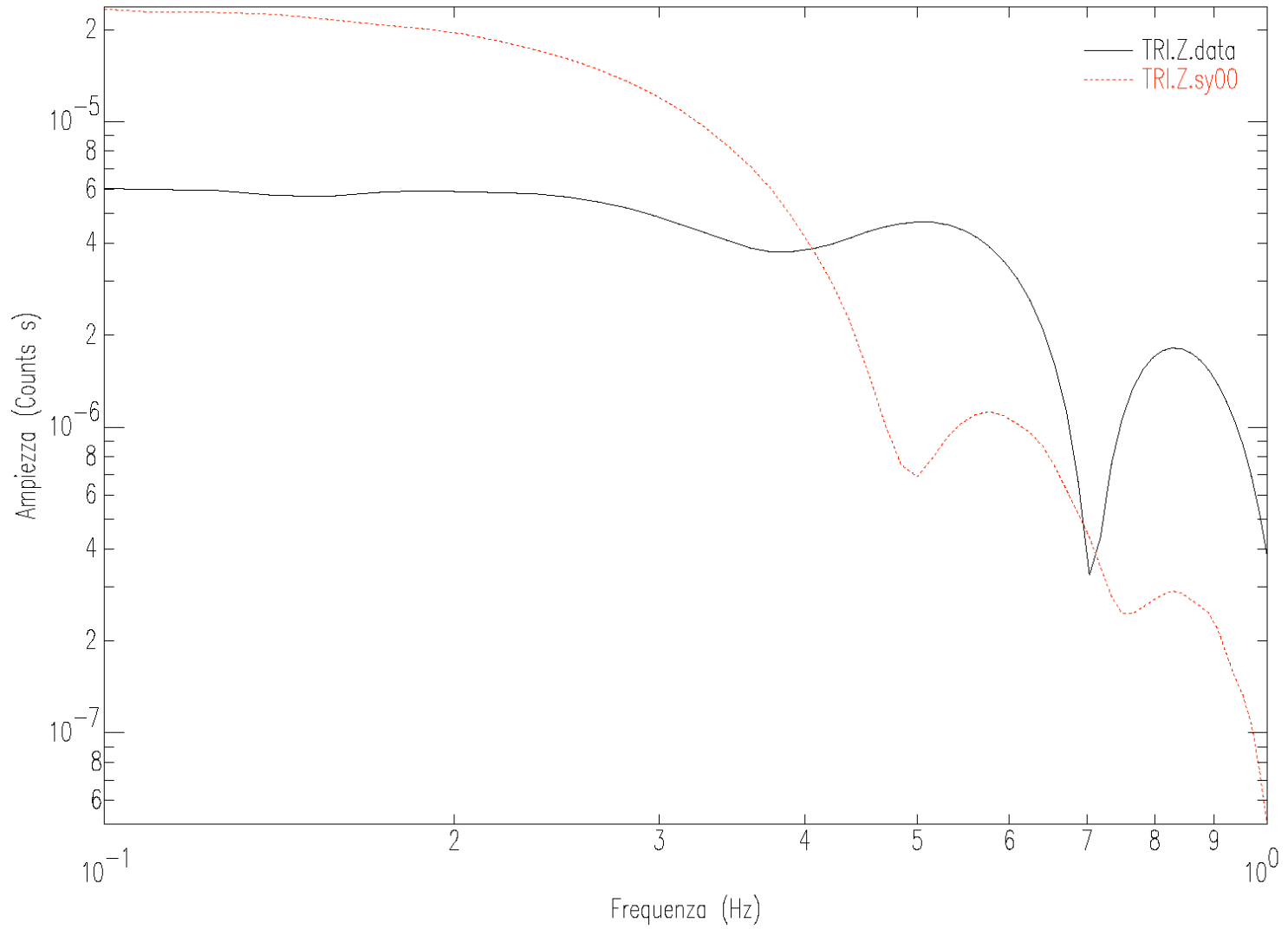
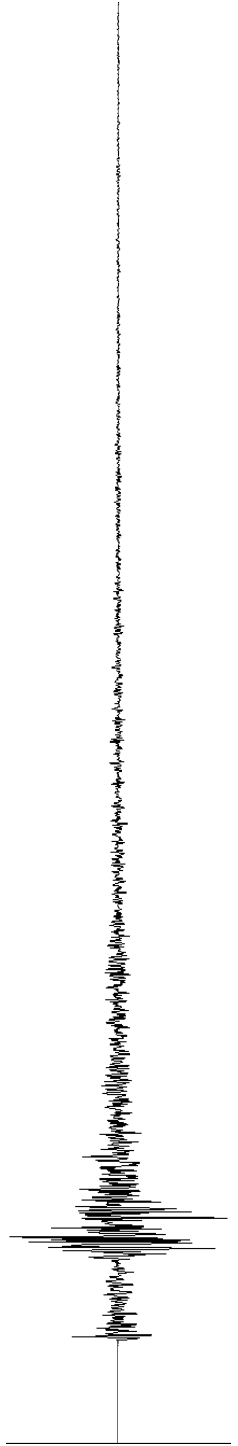
$$M_0 = \frac{4\pi r v_p^3 \rho u_0}{\Theta S_a}$$



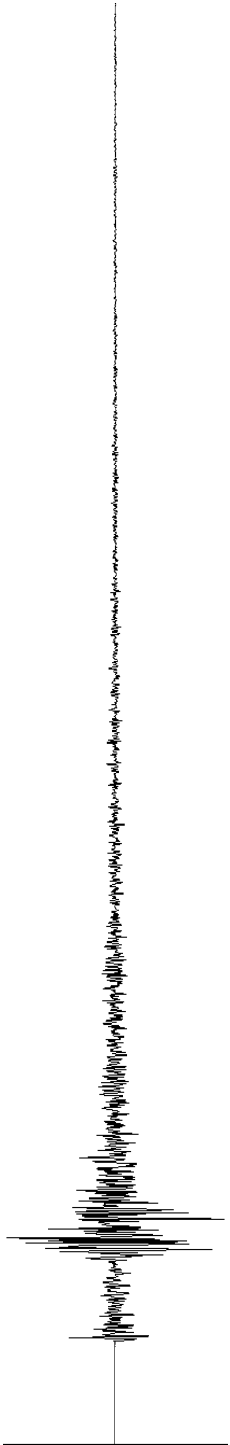
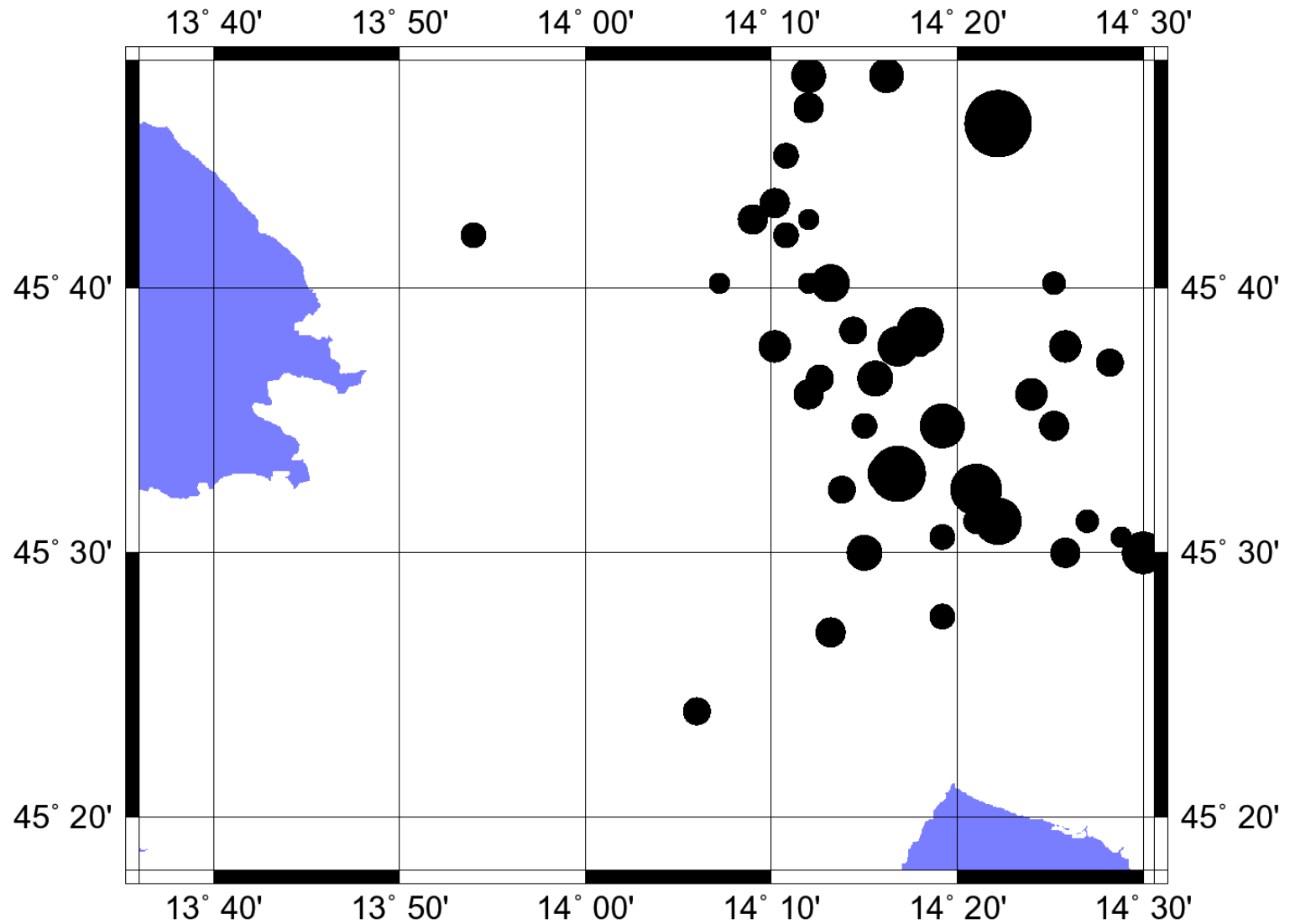
We need to compare signals for low frequencies.



Spectra comparison

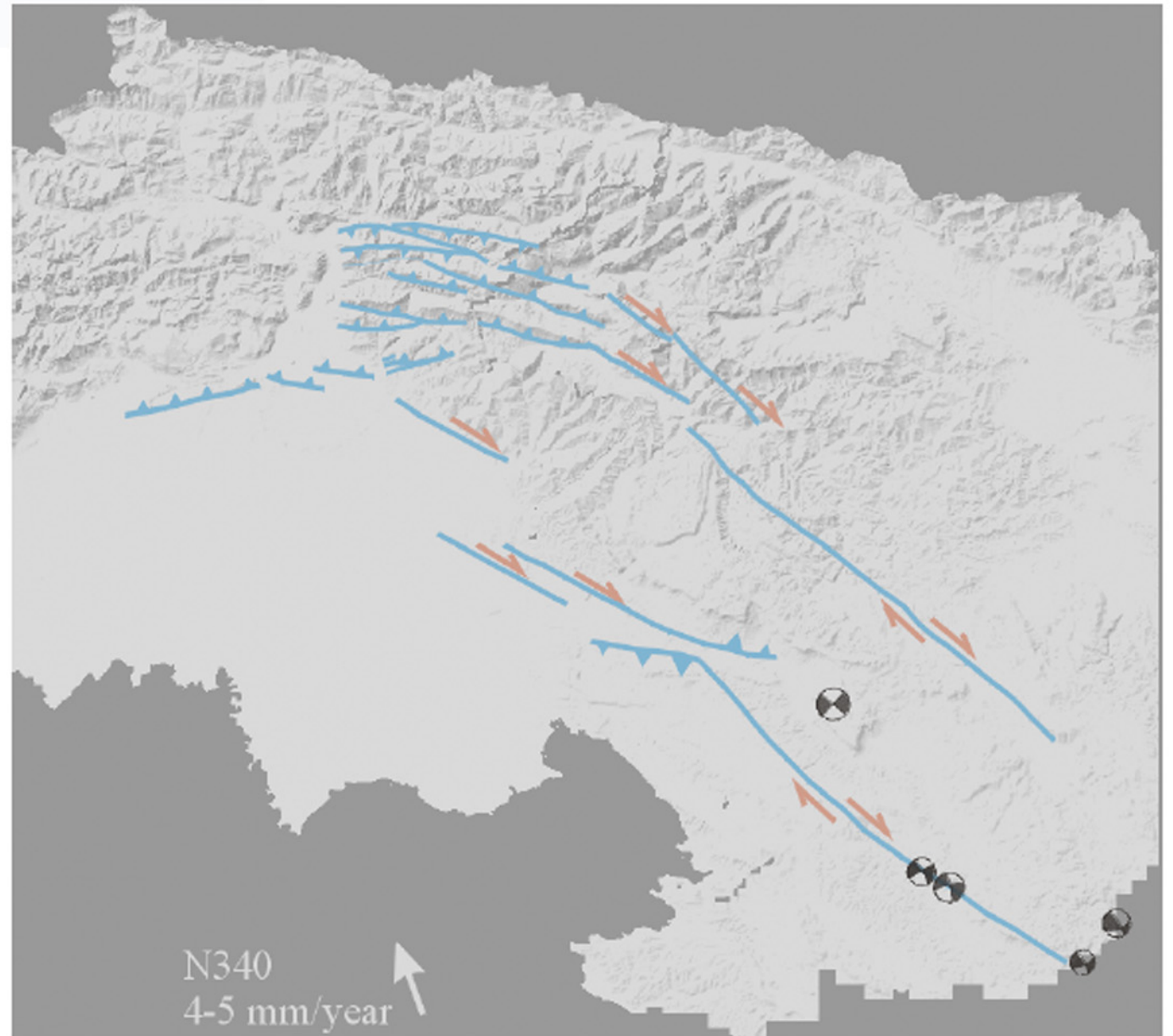


Local recent seismicity

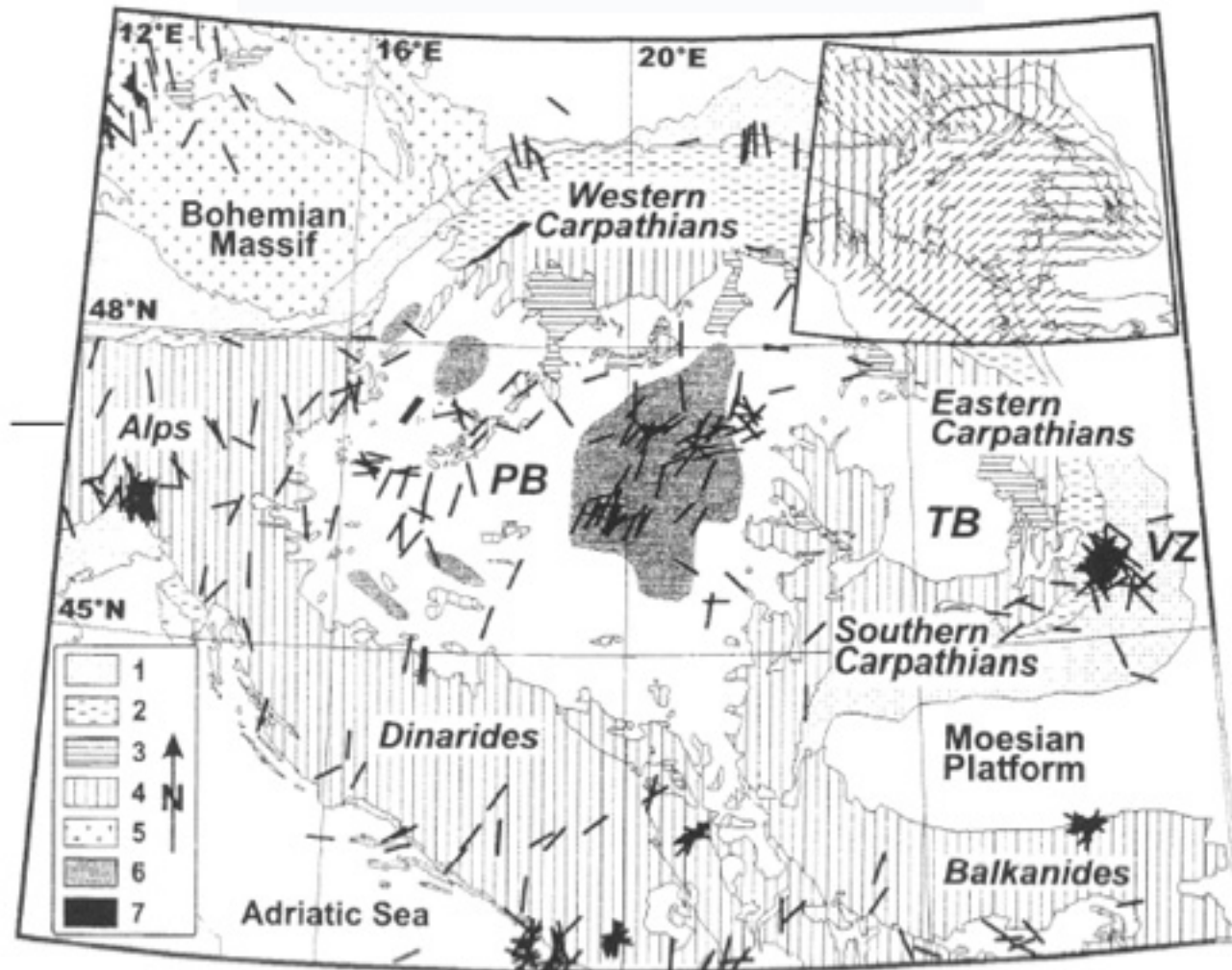


Seismotectonics and source mechanisms

Aoudia, A. (1998). Active Faulting and Seismological Studies for Earthquake Hazard Assessment, *Tesi di dottorato di Ricerca in Geofisica della Litosfera e Geodinamica*, Universit' a degli studi di Trieste.

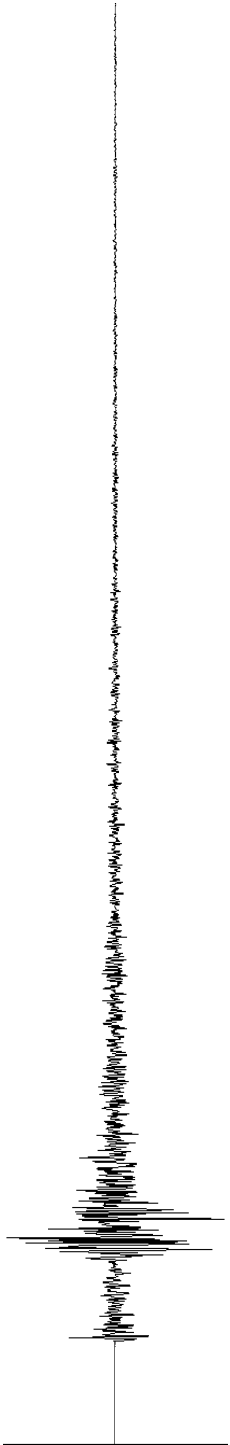
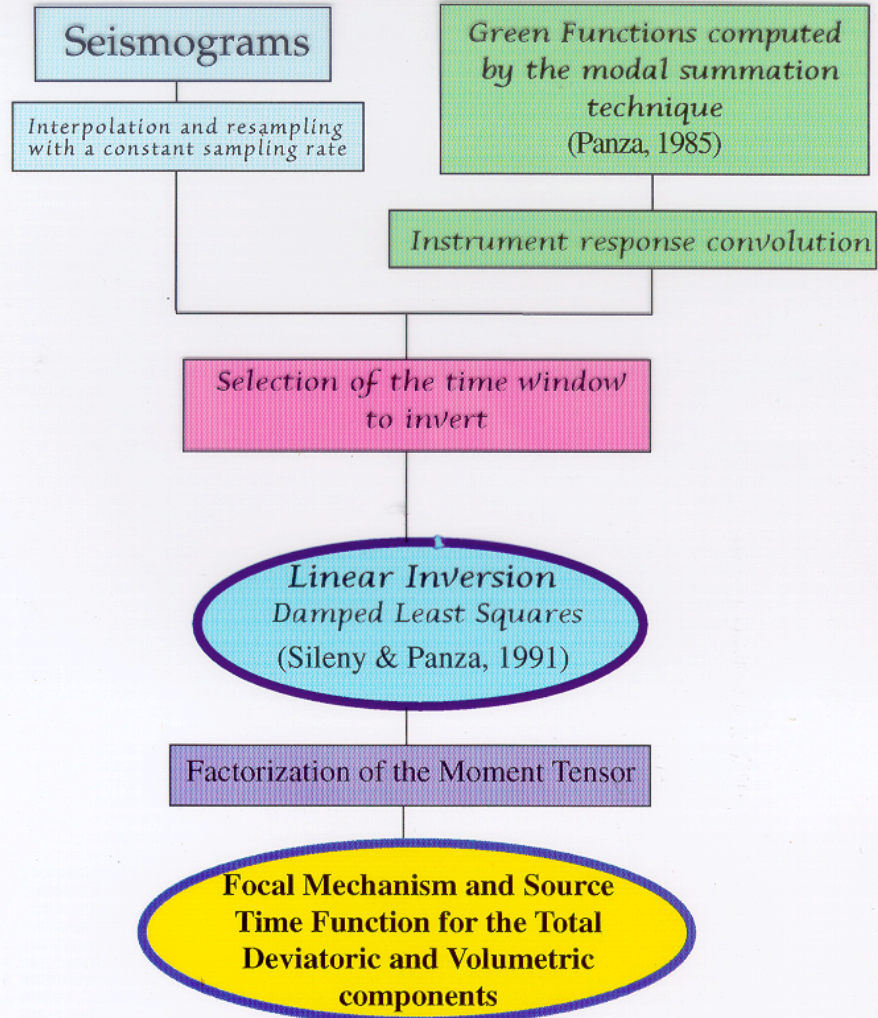


Regional stress field



Bada, G.,
Horváth, F.,
Cloeting, S.,
Coblentz, D. D.
e Tóth, T.
(2001). Role of
topography
induced
gravitational
stresses in
basin inversion:
The case study
of the
Pannonian
basin,
Tectonics, 20,
343-363.

Retrieval of Seismic Moment Tensor by Waveform Inversion



Sileny and Panza's method

(Sileny et al., GJI, 1992; 1996)

The method consists of two main steps:

- 1) *unconstrained linear inversion to determine, from the recorded seismograms, the six moment rate functions;*

$$u_k(t) = \dot{M}_{ij}(t) \otimes g_{ki,j}(t)$$

where the $g_{ki,j}$ is the far field term of the space derivative of the Green function

Once the Green functions are determined (Panza 1985), the MTRFs are obtained by using a parametrization of the moment rate functions by a series of triangles overlapping in their half-width (Nabelek, 1984).

- 2) *constrained non-linear inversion where the moment rate functions determined in the first step are used as data to obtain the average mechanism and the source time function.*

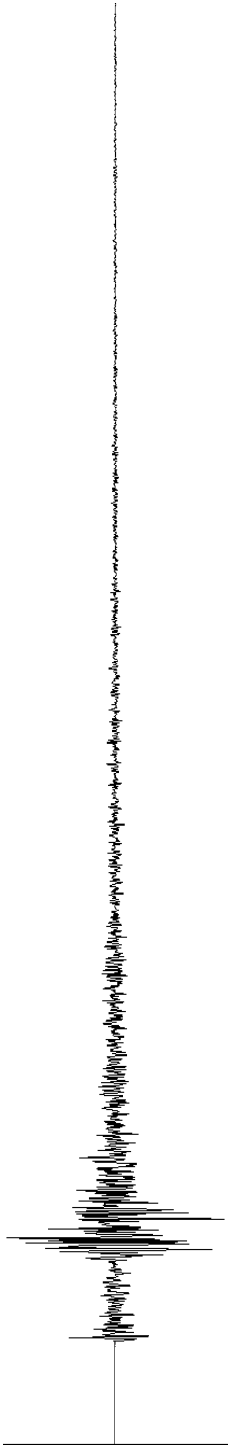
The mechanism and the source time function are obtained after factorization of the MTRFs

$$\dot{M}_{ij}(t) \rightarrow M_{ij}m(t).$$

In other words, we look for a constant MT and a common source time function. The problem is solved iteratively by imposing constraints such as

- positivity of the source time function
- a mechanism consistent with clear readings of first arrival polarities (when these are available).

The predicted MTRFs are then matched to the observed MTRFs obtained as output of the first step.



Sileny et al. (1992) method

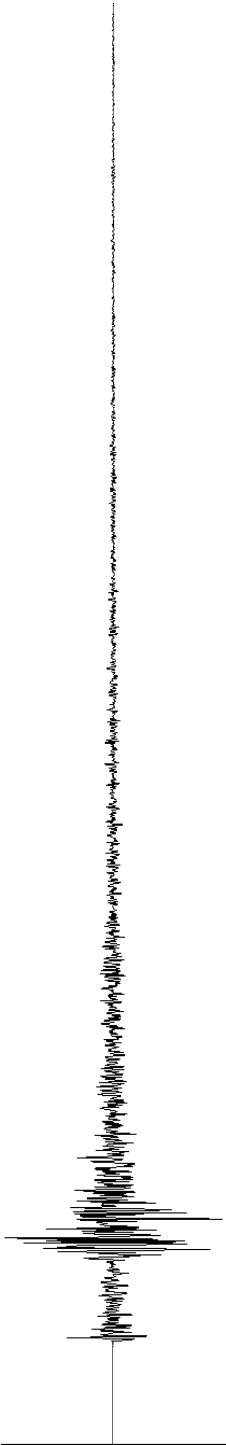
- ✓ We express displacements as

$$u_k = \sum_{i,j=1}^3 M_{ij}(t) * G_{ki,j}(t)$$

- ✓ Changing variables and differentiating

$$\sum_{p=1}^{6Nt} w_p A_{kp}(t) = d_k(t)$$

Sileny, J., Panza, G. F. e Campus, P. (1992). Waveform inversion for point source moment tensor retrieval with variable hypocentral depth and structural model, *Geophys. J. Int.* 109, 259-274.

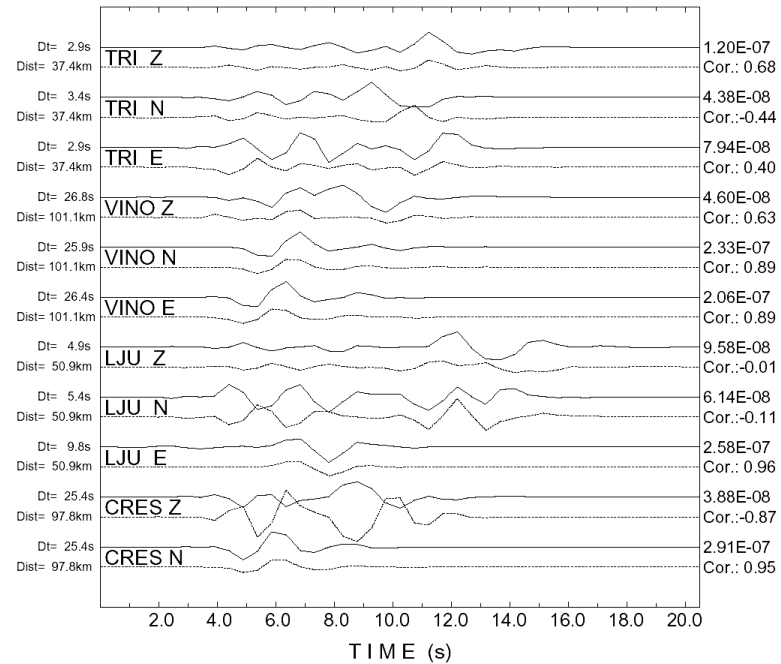


Synthetic tests

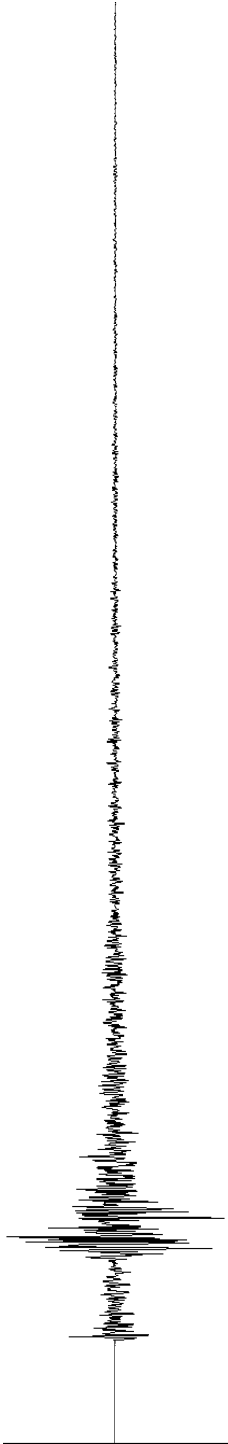
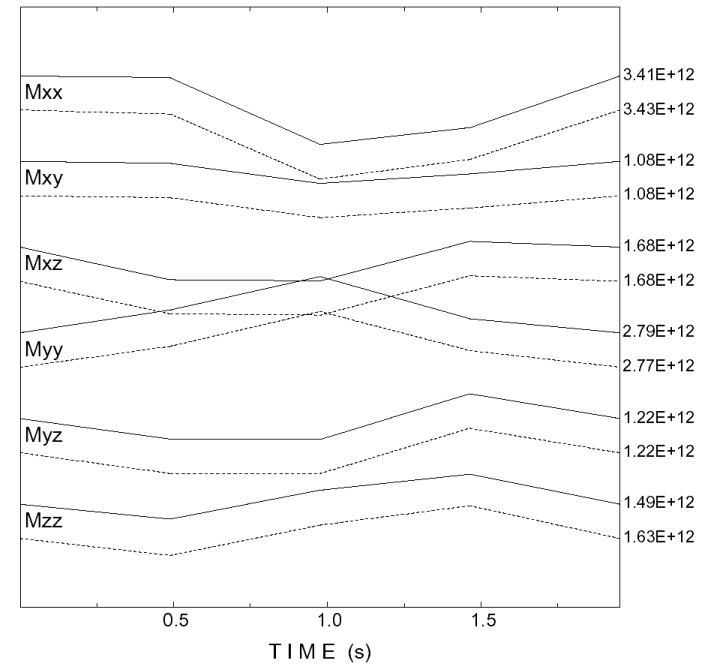
DATA FIT - Normalized Correlation: 0.36

Mij' TIME VARIATION

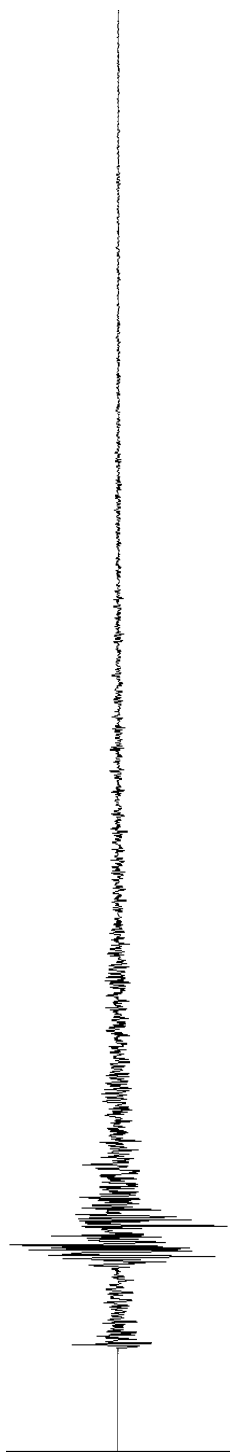
Observed and Synthetic Data



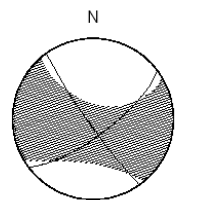
Full and Deviatoric Moment Rates (Nm/s)



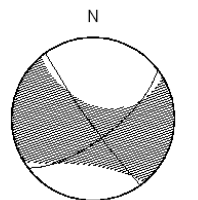
Synthetic tests



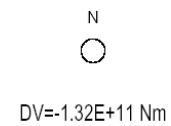
MOMENT TENSORS



53 73 -6 / 145 85 -163
 $M_0 = 6.12E+12$ Nm

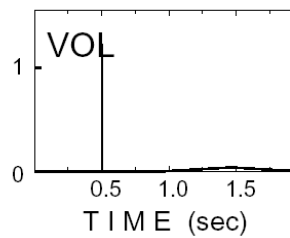
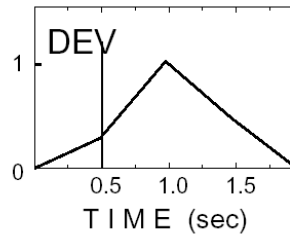
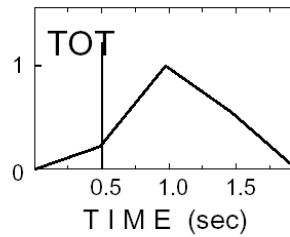


53 70 -5 / 144 86 -160
 $M_0 = 6.25E+12$ Nm



DV=-1.32E+11 Nm

SOURCE TIME FUNCTIONS



RMS of factorization &
Correlation with polarities

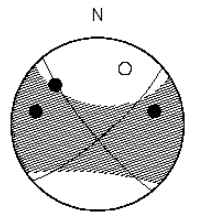
RMS: 0.4890
Correl: 0.000

RMS: 0.4369
Correl: 0.000

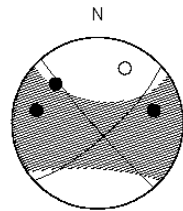
RMS: 0.6105
Correl: 0.000

Real data


MOMENT TENSORS



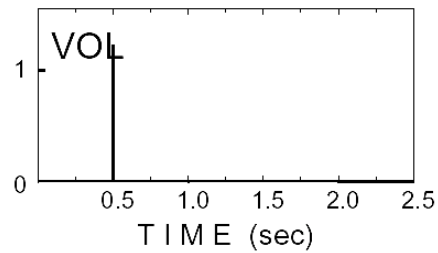
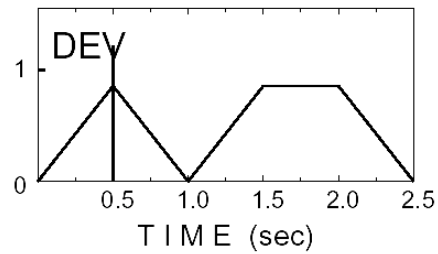
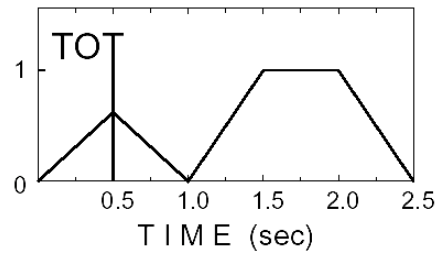
49 79 -9 / 141 81 -168
 $M_0 = 5.77E+14$ Nm



48 77 -4 / 139 86 -167
 $M_0 = 5.68E+14$ Nm


 $DV = -2.83E+12$ Nm

SOURCE TIME FUNCTIONS

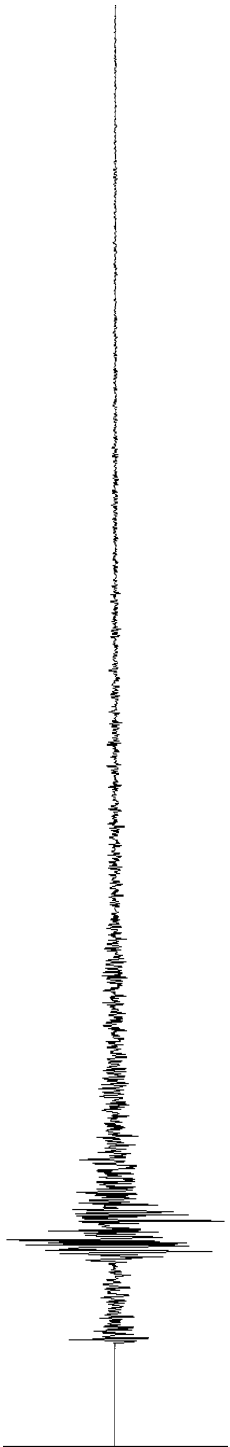


RMS of factorization &
Correlation with polarities

RMS: 0.7755
Correl: 0.776

RMS: 0.7739
Correl: 0.803

RMS: 0.0000
Correl: -0.500



CAMPI FLEGREI EVENT (Campus et al., 1993)

20/03/84 (2.5,5.,.5) I

M.R.C.

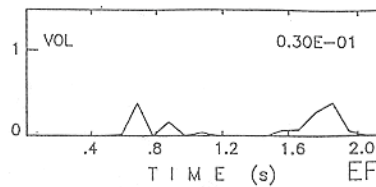
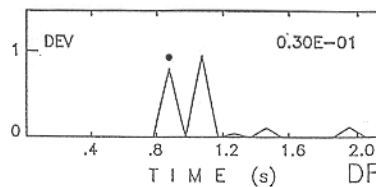
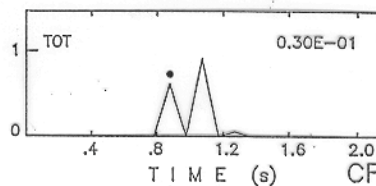
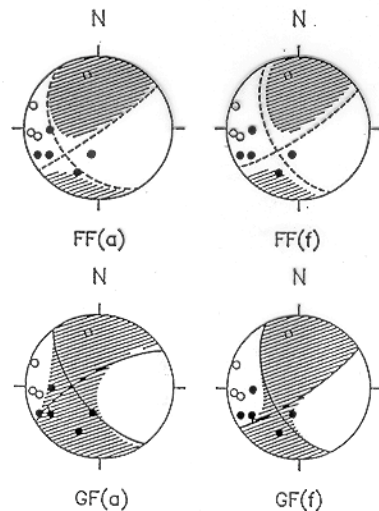
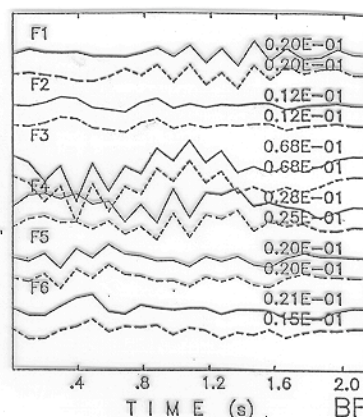
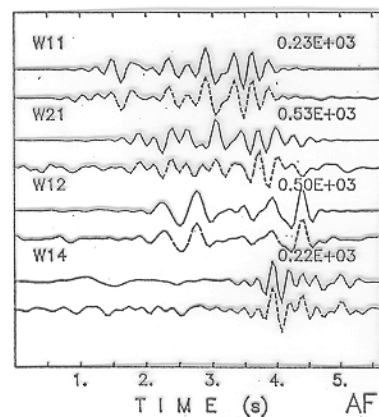
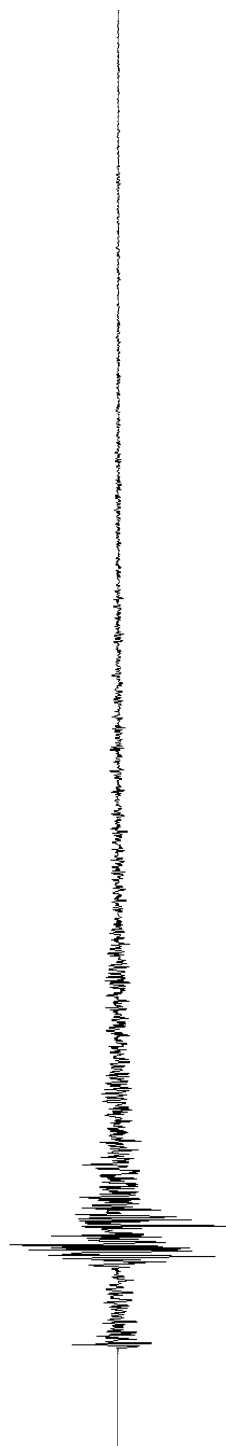


Fig. 5.7. Evento del 20/03/84, h. 21:21:34.03; 5Hz.

A: linea continua: dati; linea tratteggiata: sismogrammi sintetici; in alto a sinistra: sigle delle stazioni; in alto a destra: ampiezze massime relative dei dati reali. B: M.R.C.=Moment Rate Components: elementi (F1...F6) della derivata del tensore momento sismico completo (T) (linee continue) e della sua parte deviatoria (D) (linee tratteggiate). C: funz. temporale di sorgente comune ai sei elementi del tensore T. D: funz. temporale di sorgente comune ai 6 elementi del tensore D. E: funz. temporale di sorgente comune ai 6 elementi del tensore isotropico V. F: (a) mecc. medio e (f) dedotto dal primo picco significativo (*) del tensore T. G: (a) mecc. medio e (f) dedotto dal primo picco significativo (*) del tensore D. Sono sovrapposte le letture delle polarità: cerchi pieni: compressioni, cerchi vuoti: dilatazioni.



Why do retrieve the seismic moment tensor?

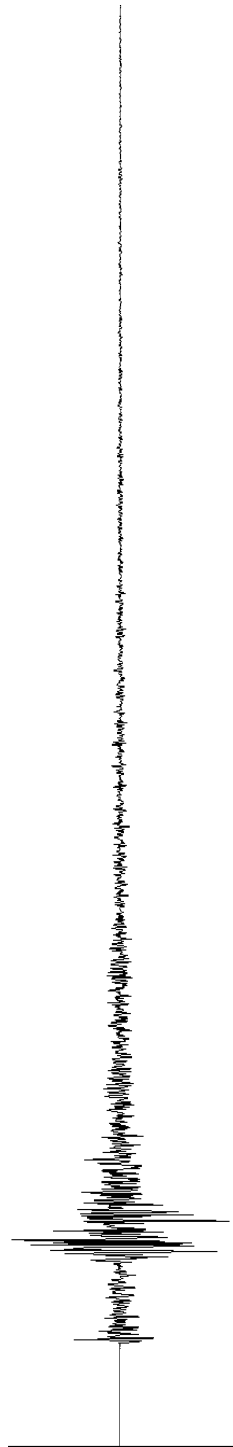
The seismic moment tensor is retrieved by waveform inversion and does not require a priori constraints on the source approximation.

This means that ...

it is very suitable to study weak events which are typical of volcanic areas being, such approach, poorly affected by all those factors

- (- low energy content,*
- improper force equivalent source approximation,*
- noise contamination of the data*
- small number of recording stations)*

which prevent the methodologies based on first arrivals polarities to get reliable results.



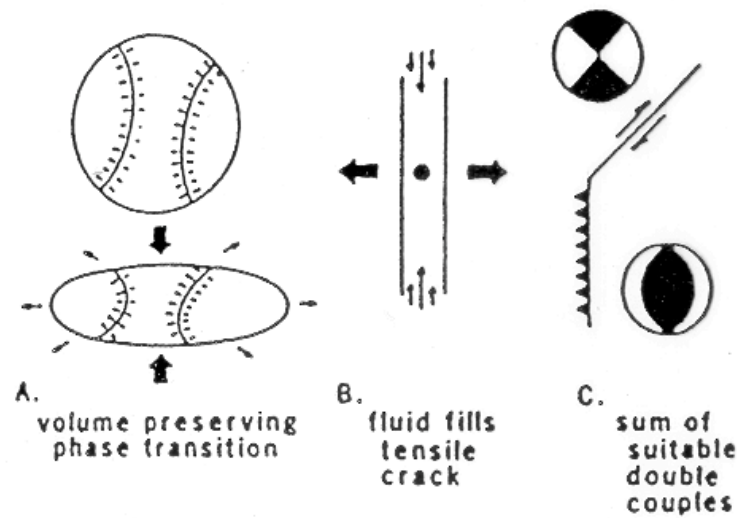


Fig. 1. Suggested models for a CLVD source: For a pure CLVD source particle motion is inward (outward) along one axis, and outward (inward) along the two normal axes, with no net volume change. This might occur; (a) if a phase change caused a spherical volume to become disk-shaped, with no net change in volume; (b) when fluid suddenly fills a tensile crack; and (c) if two double-couple earthquakes occur simultaneously. The resulting source is a pure CLVD if they have the same size, and if they have parallel P (or T) axes and perpendicular B axes. Here the focal mechanisms and faults are shown in map view.

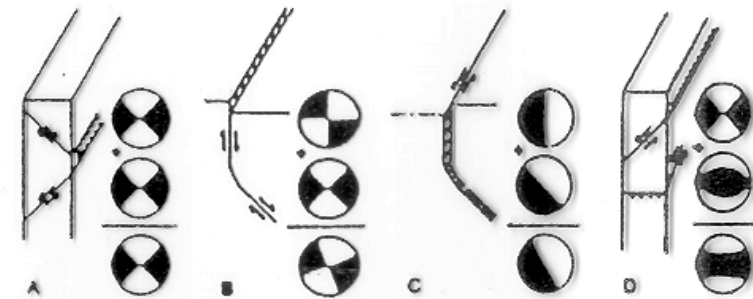
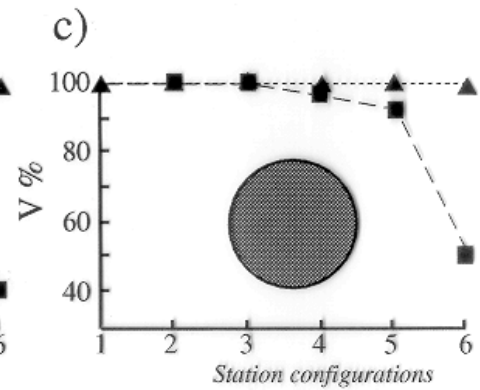
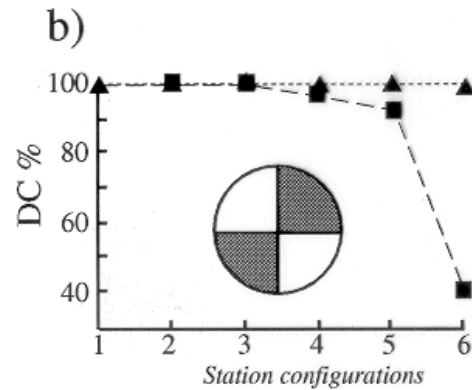
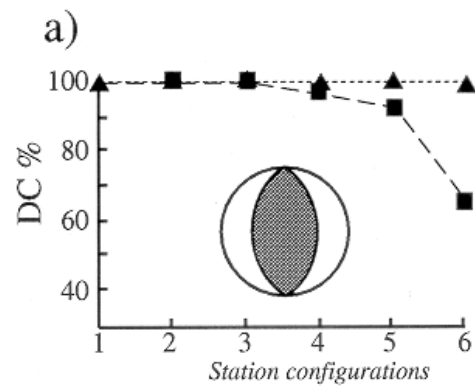
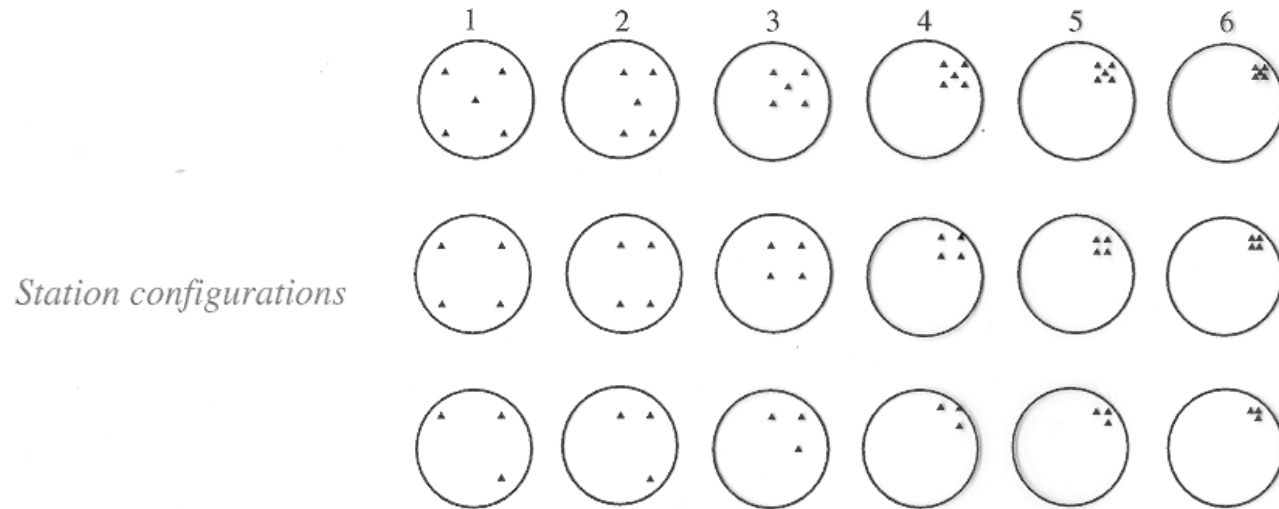


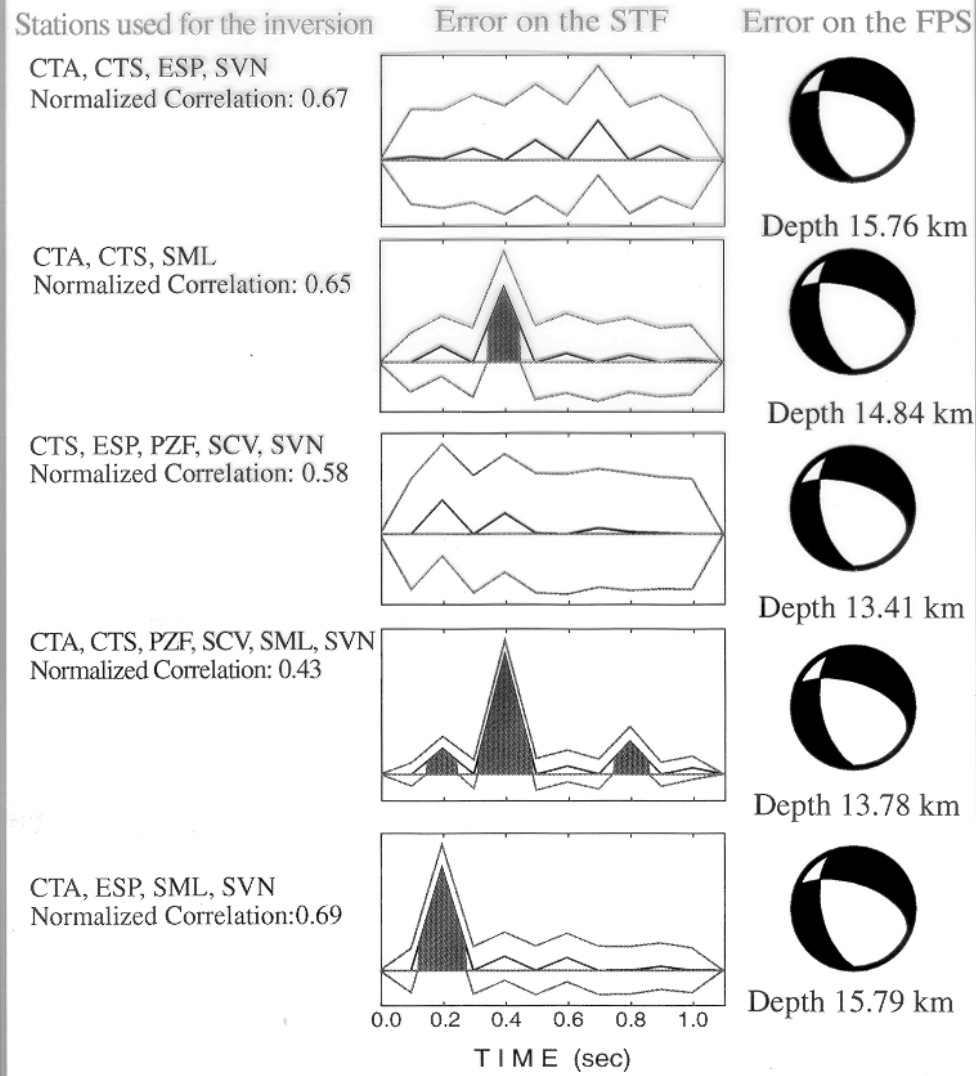
Fig. 2. The sum of pure double-couple subevents may produce a source which is a pure double couple, a pure CLVD, or any combination in between. Thus subevents with the same B-axes, as in (a) or (b), or subevents with the same slip vectors, as in (c), produce a pure double couple. However, subevents having the same P axes but perpendicular B axes add to form a pure CLVD event. Such a P_{edge} source pattern might occur at the edge of a subducting lithospheric slab. In this figure the focal mechanisms are shown as back-hemisphere projections.

Effects of the station distribution



(from Sileny et al., 1996)

Inversion with different groups of stations



Depth 15.76 km

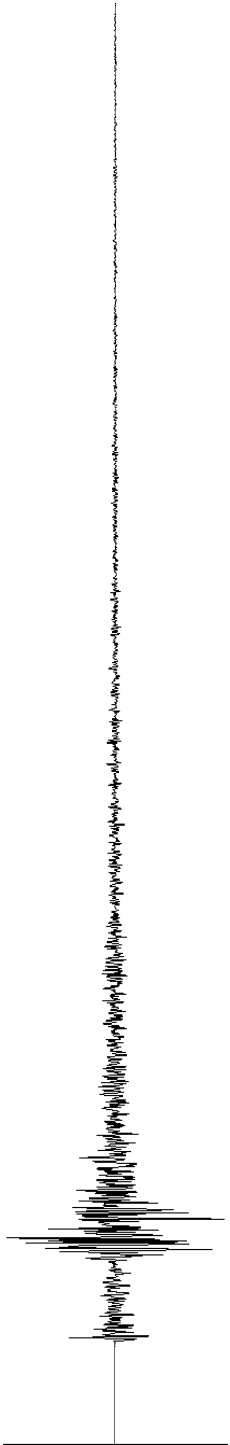
Depth 14.84 km

Depth 13.41 km

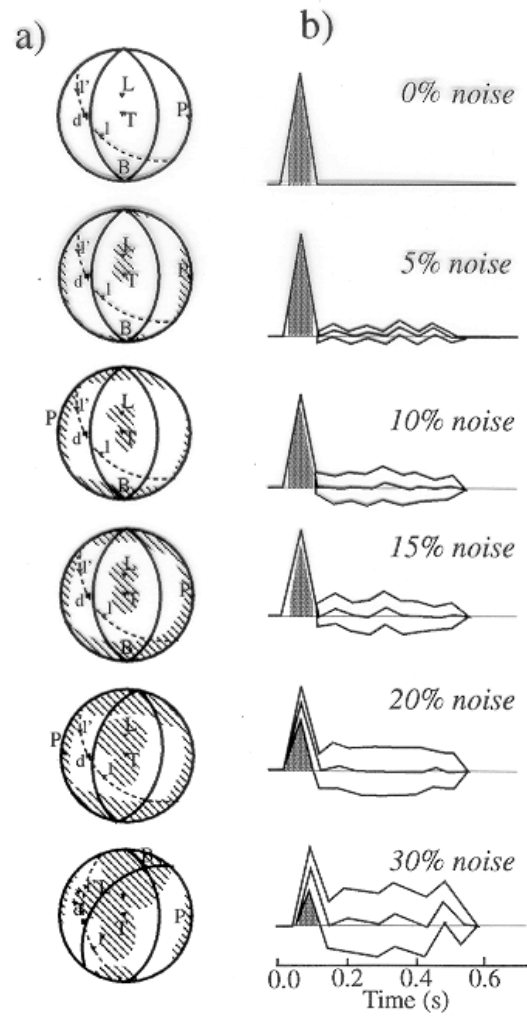
Depth 13.78 km

Depth 15.79 km

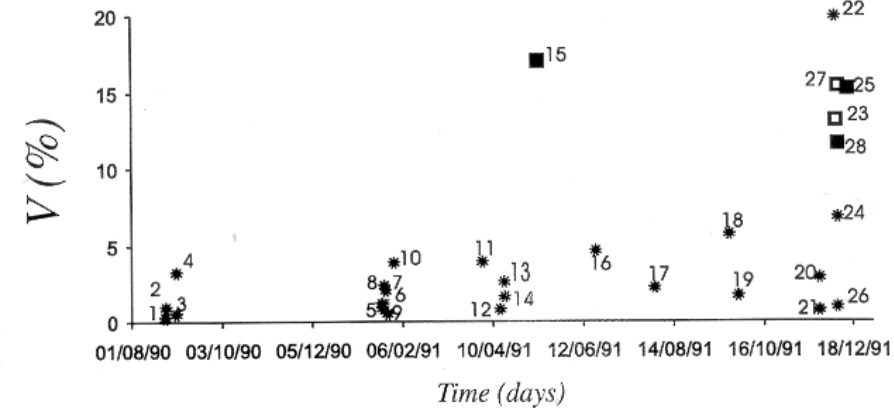
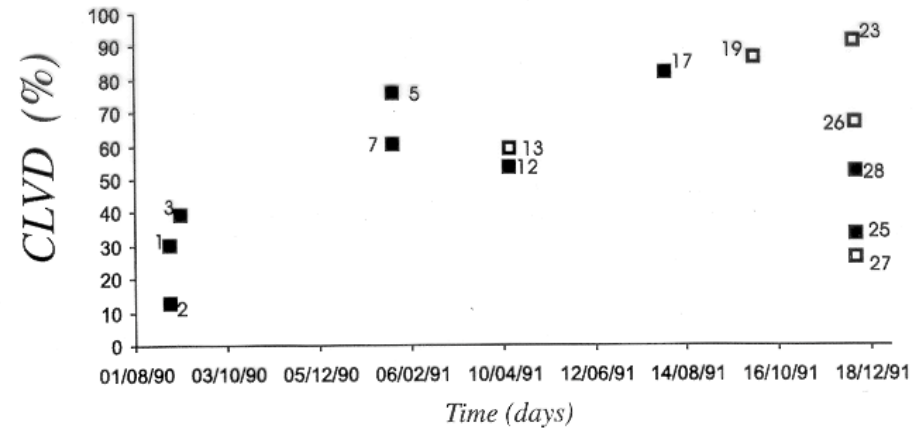
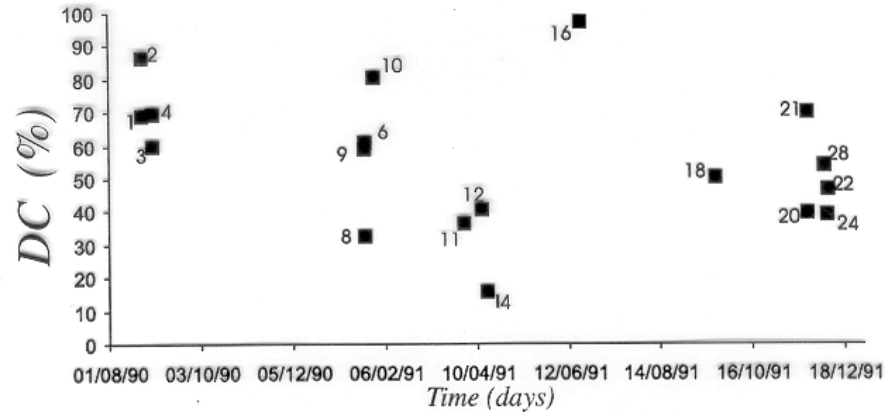
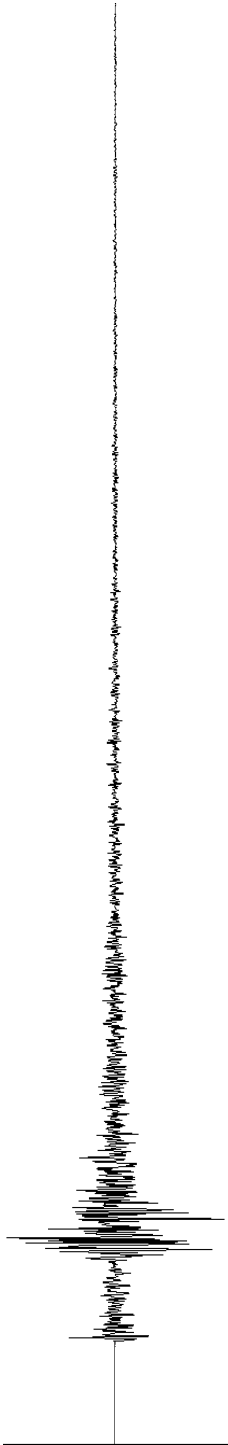
ICTP 2004



Effects of noise



(from Sileny et al., 1996)



Seismicity of Mt. Etna

Advantages and limits of the method

Several tests have been performed to test the robustness of the Sileny and Panza method as well as comparisons with other source inversion procedures. We observed that

it is not necessary to fix the source model a priori

only 4 recording stations are enough to retrieve the moment tensor components

the method well copes with structural heterogeneities.

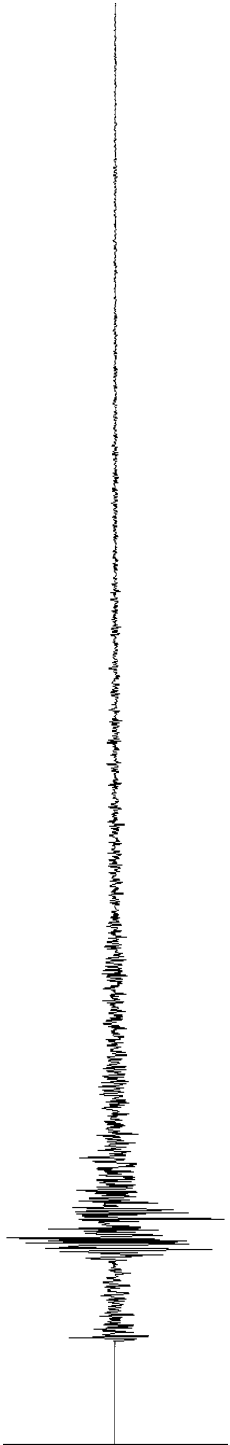
BUT...

What is the influence of the damping value on the results?

What is the reliability of the isotropic component?

What is the influence of heterogeneities in a volcanic environment on the inversion results?

What is the effect of the station distribution?



CONCLUSIONS

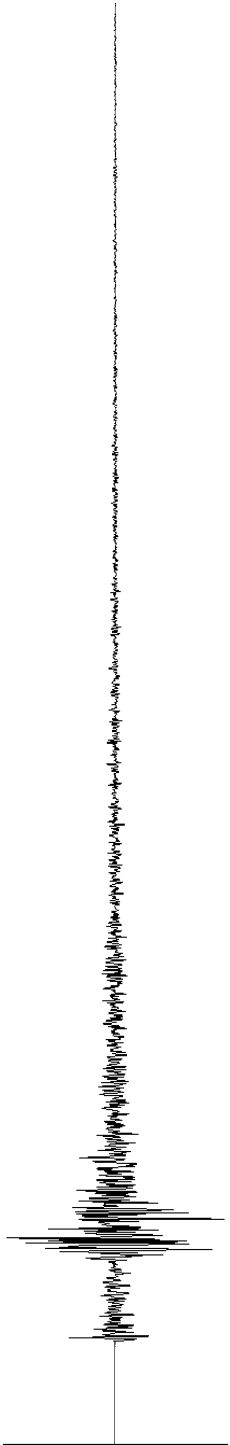
We show by synthetic tests that, by an appropriate error analysis of the results, false non-double couple due to

- 1) poor station coverage
- 2) mislocation of the hypocentre
- 3) noise contamination of the data
- 4) inadequate structural modeling

can be recognized in the moment tensor solution.

The analysis is even more robust when in the same region the evolution in time of the non-double couple components is investigated.

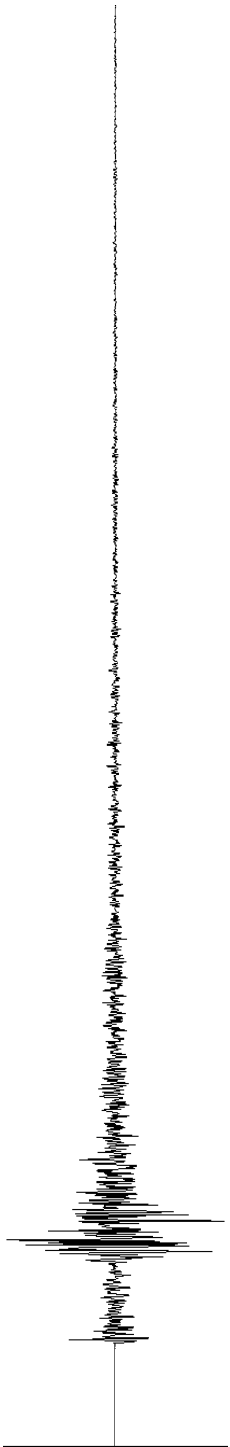
Since spurious non-double couple components can arise just because of the station configuration, when dealing with real data any inversion must be preceded by synthetic tests to define lower limits above which the non-double couple components found can be considered statistically significant at a certain confidence level.



The full moment tensor retrieval is a really suitable approach to study volcanic seismicity.

The tests of robustness of the Sileny Panza method show up that:

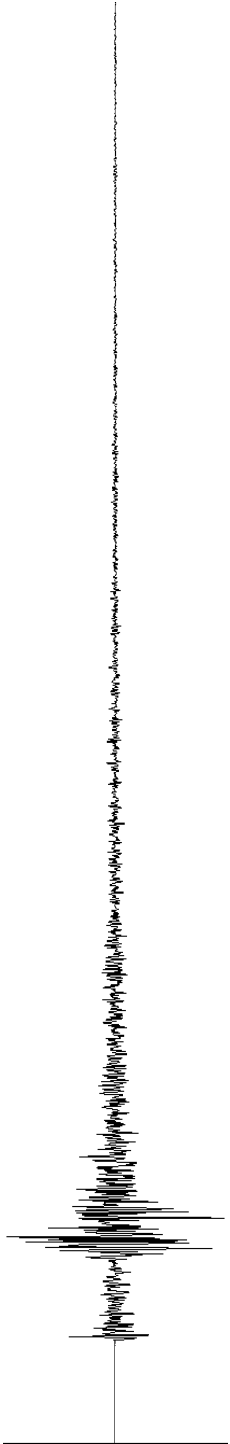
- the method well copes with effects of structural heterogeneities or with effects due to the poor knowledge of the medium
- there is coincidence between the FPS computed by first arrivals and by our inversion when the mechanism has a very high percentage of Double Couple and a negligible Volumetric Component
- the resolution for the isotropic component is quite reliable.
- All the above results have been confirmed by applying the method in tectonic environments (Vrancea, Friuli Venezia Giulia, Umbria-Marche) and geothermal regions (Larderello, Italy).



Waveform inversion

Finite fault case

Problem of inverting recorded ground motion time series for the seismic source rupturing process on finite faults.



Waveform inversion

Given the time series of motion recorded at a certain number of station around the causative fault, find the temporal and space distribution of slip on the finite fault.

Past studies until some time ago have concentrated on deriving a model that fits the data, without assessing solution stability or resolution.

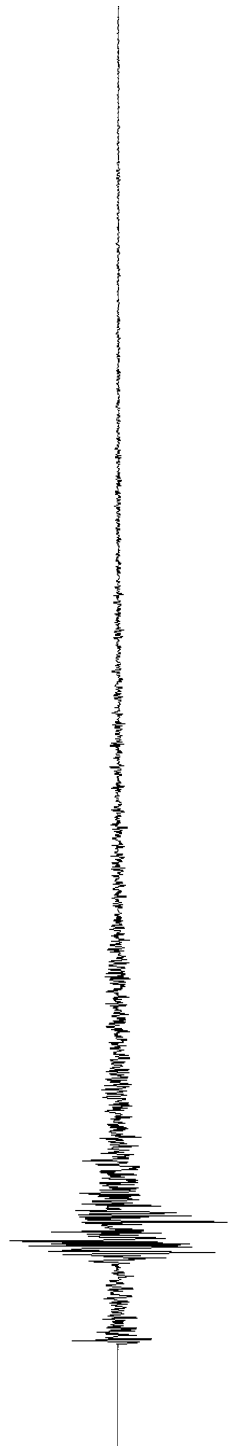
Using standard inverse methods it is not difficult to obtain a solution which fits the data acceptably well.



Waveform inversion

Assumption

An earthquake starts at a point and grows outward with a **continuous rupture**, i.e. the rupture may not jump. This last condition may be relaxed at predetermined fault segments.



Forward problem

Displacement at a station is given by

$$u_k(\mathbf{x}_1, t_1) = \int_0^{t_1} dt \iint_{\Sigma} K_{ik}(\mathbf{x}_1, \mathbf{x}; t_1, t) a_i(\mathbf{x}, t) dS$$

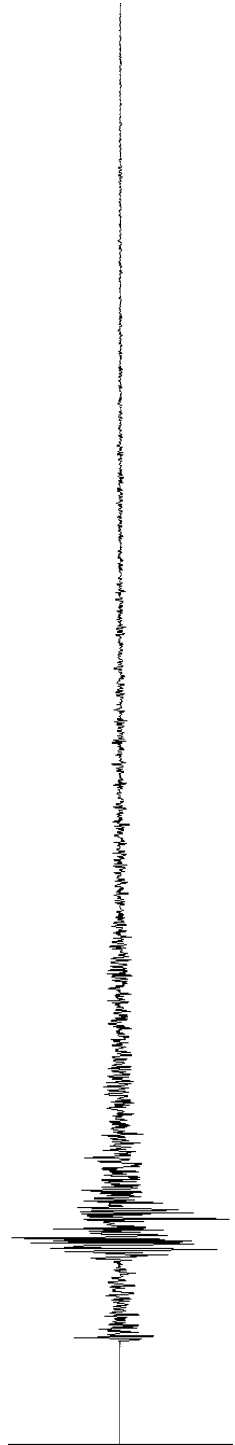
where

u_k = k-th component of displacement at (\mathbf{x}_1, t_1)

K_{ik} = impulse response of the medium

$a_i(\mathbf{x}, t)$ = slip at (\mathbf{x}, t) on fault

Σ = fault area



Forward problem

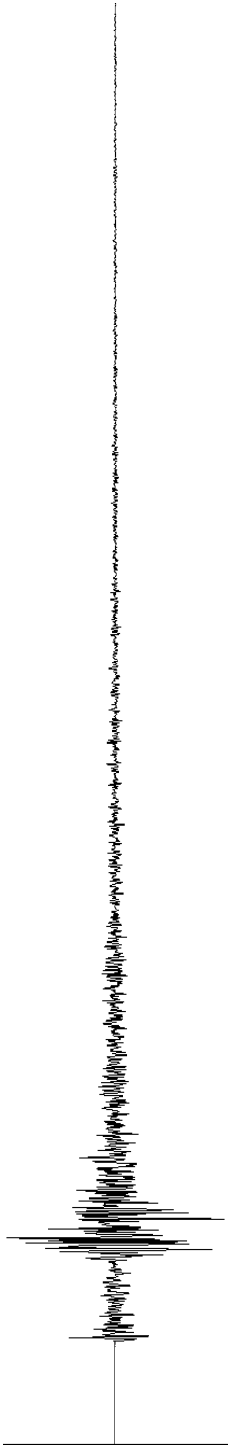
After some simple algebra (move derivative from K to a in convolution) we get:

$$S_j(t_1) = \int_0^{t_1} dt \iint_{\Sigma} W_j(\xi; t_1 - t) \dot{a}_i(\mathbf{x}, t) dS$$

S_j = seismogram at j -th station at time t_1 - DATA

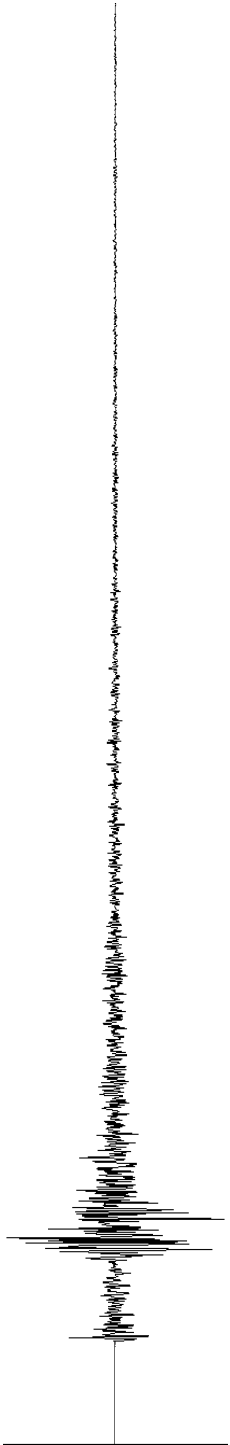
W_j = impulse response; direction of slip is taken
to be constant and parallel to the applied stress
direction - KNOWN

$\dot{a}(\mathbf{x}, t)$ = slip rate at (\mathbf{x}, t) on fault - UNKNOWN



Forward problem

- The fault is discretized. In each cell of size $\Delta x \Delta y$, \dot{a} is a linear function
- W_j is discretized by integrating over cells
- The source time function is discretized by taking a fixed time step Δt and assuming slip rate varies linearly with time.



Forward problem

Then, in discrete form we get the system of linear equations

$$\mathbf{A} \mathbf{x} = \mathbf{b}$$

\mathbf{A} = discretized impulse response W_j

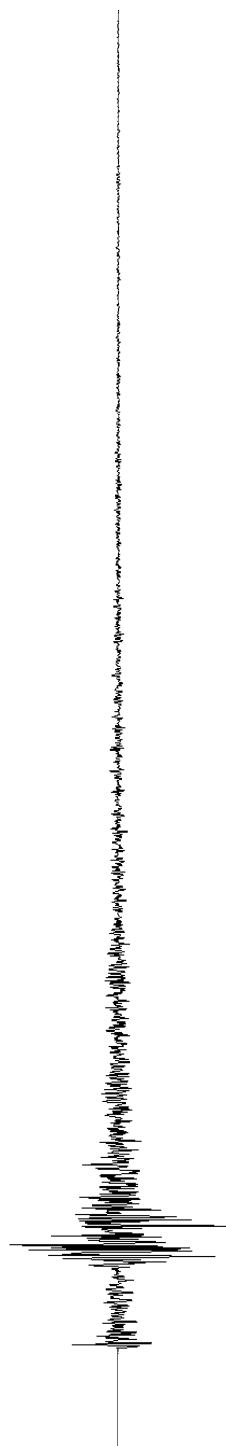
\mathbf{x} = unknown slip rates \dot{u}

\mathbf{b} = data from seismograms

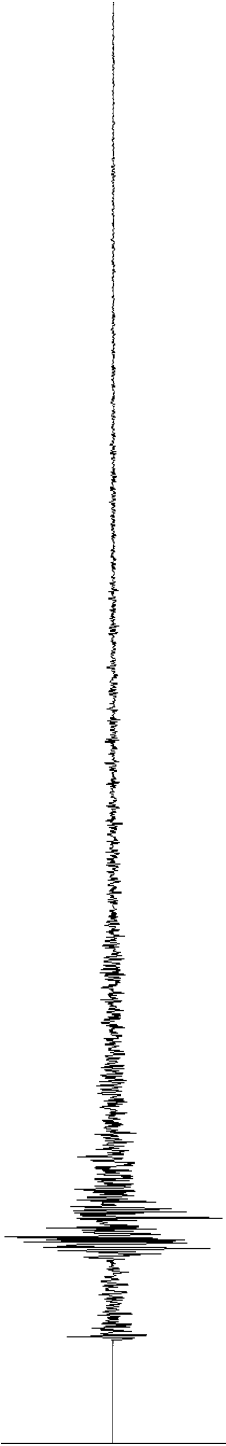
Number of equations = (# of grids along x) x

(# of grids along y) x

(# of source time steps)



Set up matrix equation



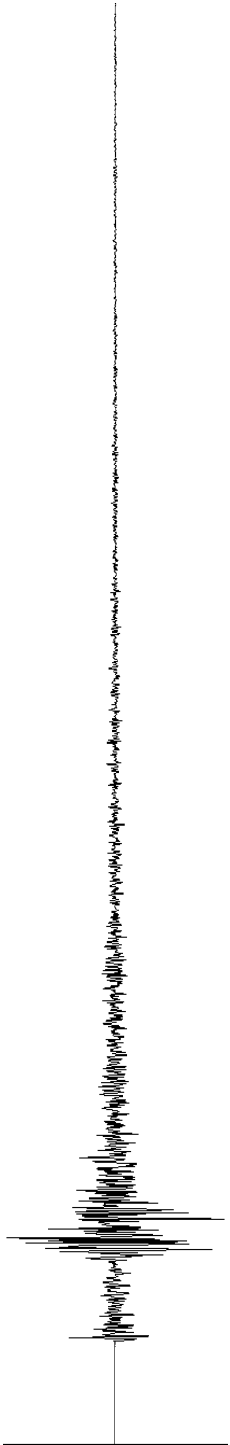
$$\begin{bmatrix}
 \left. \begin{matrix} \text{Time points for station 1} \\ \cdot \\ \cdot \\ \cdot \end{matrix} \right\} & \left. \begin{matrix} \text{subfault 1 synthetics} \\ A_{11} & A_{12} & \cdot & \cdot & \cdot & A_{1m} \\ A_{21} & A_{22} & \cdot & \cdot & \cdot & A_{2m} \\ \cdot & \cdot & & & & \\ \cdot & \cdot & & & & \end{matrix} \right\} \\
 \left. \begin{matrix} \text{Time points for station 2} \\ \cdot \\ \cdot \\ \cdot \end{matrix} \right\} & \\
 \left. \begin{matrix} \text{Time points for station k} \\ \cdot \\ \cdot \\ \cdot \end{matrix} \right\} & \\
 \left. \begin{matrix} A_{n1} & A_{n2} & \cdot & \cdot & \cdot & A_{nm} \end{matrix} \right\}
 \end{bmatrix}
 \cdot
 \begin{bmatrix}
 X_1 \\
 X_2 \\
 \cdot \\
 \cdot \\
 \cdot \\
 X_m
 \end{bmatrix}
 \begin{matrix}
 \text{Dislocation on subfault 1} \\
 \text{Dislocation on subfault 2} \\
 \\
 \\
 \\
 \text{Dislocation on subfault m}
 \end{matrix}
 \approx
 \begin{bmatrix}
 \left. \begin{matrix} \text{Data} \\ \text{time points for station 1} \\ b_1 \\ \cdot \\ \cdot \end{matrix} \right\} \\
 \left. \begin{matrix} \text{Data} \\ \text{time points for station 2} \\ \cdot \\ \cdot \end{matrix} \right\} \\
 \left. \begin{matrix} \text{Data} \\ \text{time points for station k} \\ \cdot \\ \cdot \end{matrix} \right\} \\
 \left. \begin{matrix} b_n \end{matrix} \right\}
 \end{bmatrix}$$

Possible physical constraints

1. Limit on fracture propagation speed
2. Direction of slip vector on fault is parallel to direction of the average stress drop

Leads to the “no back-slip” constraint

3. Max. slip rate on the fault can be constrained based on fracture mechanics results from laboratory experiments on rocks



Constraints

1. No back-slip, i.e. $x \geq 0$ always
2. Causality constraint: grids not allowed to slip until first wave from point of rupture initiation arrives

STRONG CAUSALITY CONSTRAINT

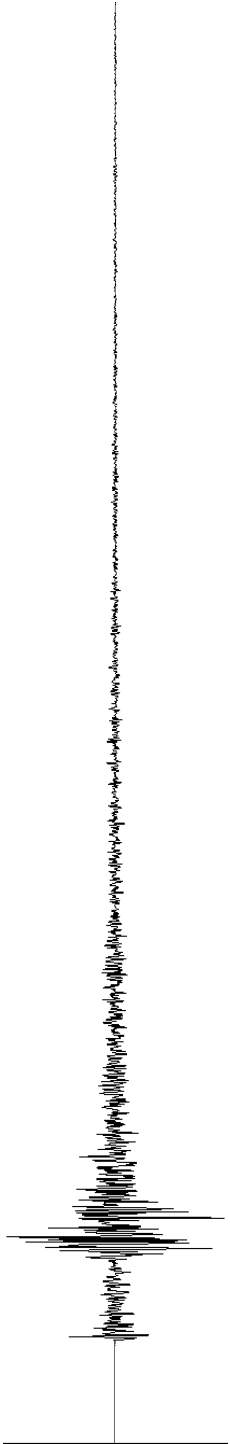
3. Seismic moment constraint

The seismic moment resulting from the solution must be consistent with that obtained from long-period data (e.g. CMT solution)

$$\sum c_i x_i = M_0$$

Summed over fault with c_i containing rigidity modulus
etc.

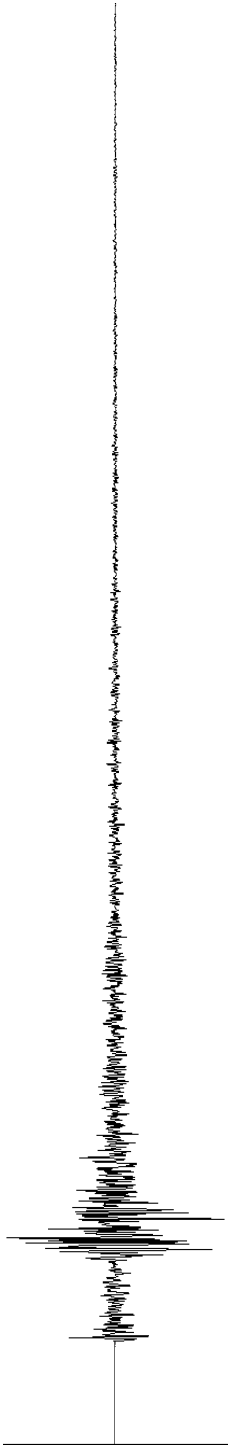
ICTP 2004



Acceptable solutions

In order for a particular slip distribution to be an acceptable solution to the inverse problem it must satisfy the following three conditions:

1. The solution must explain the data
2. The solution must be physically reasonable
3. If more than one solution fits the data equally well, additional information must be supplied to uniquely define which solution is being obtained and **such constraints should be explicitly stated and not hidden in the method of inversion.**

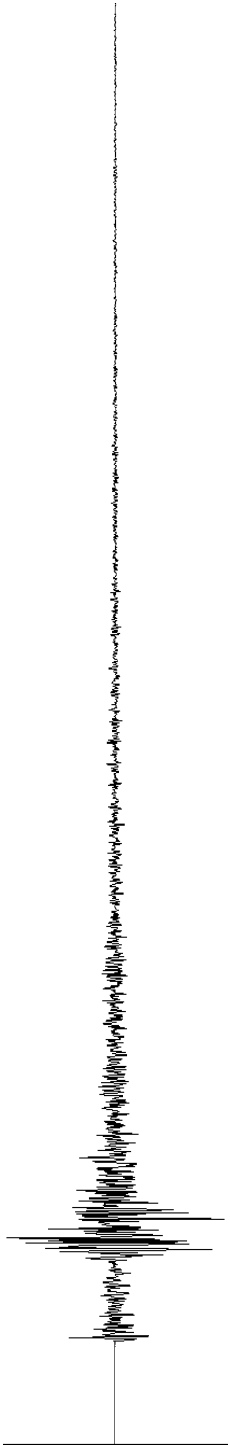


Waveform inversion

Size of the cell

The rupture surface is subdivided into a grid work of small cells or subfaults.

They should be small enough in order for the solution to outline well the rupturing process, but on the other end as the number of cells increases, the stability of the problem decreases. The point-source spacing is such that the subfault synthetics look like a continuous rupture over the bandwidth of the inversion and not as a bunch of separate point-source releases. This is obviously related to the minimum wavelength one wants to resolve in the problem or equivalently to the maximum frequency involved.

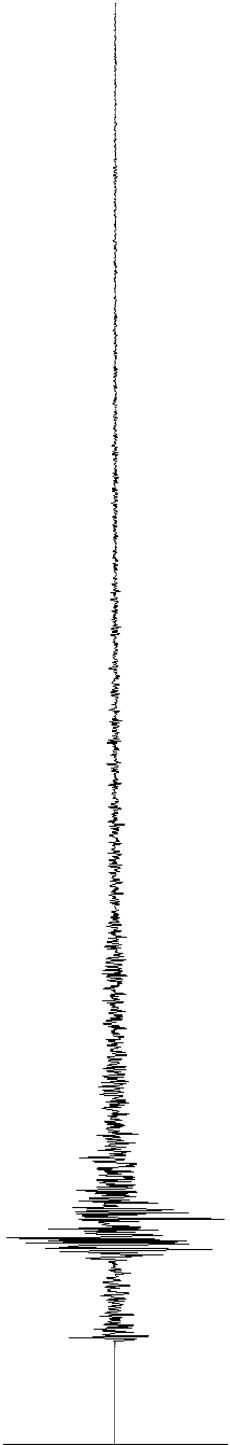


Waveform inversion

Cells should be small enough in order for the time required to the rupture to traverse a subfault be significantly less than the predominant period content of the data.

However also the directivity effect is important and a good check is therefore to make forward models with smaller and smaller cells until the seismograms at the given stations are stable.

If the subfault synthetics are computed before the inversion process is initiated, the speed of inversion increases significantly.

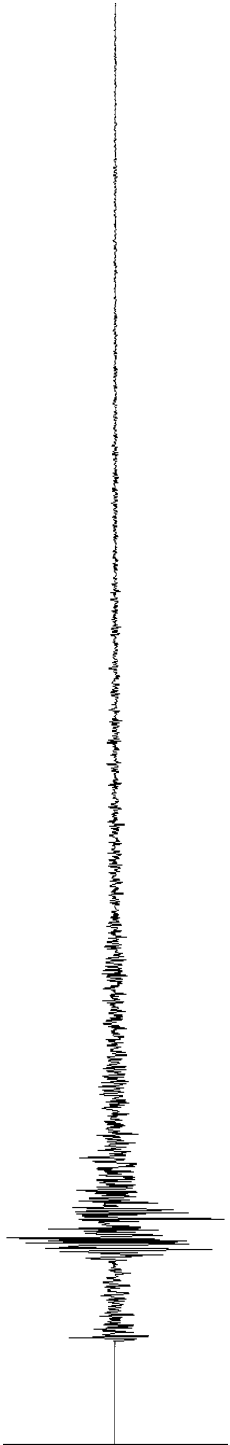


Waveform inversion

The ground motion for a unit amount of slip on each subfault is computed by a time-domain sum of point sources.

Rupture velocities: range from 2 km/s to 4 km/s.

Each subfault synthetic is lagged in time and scaled in amplitude according to the present model estimation.

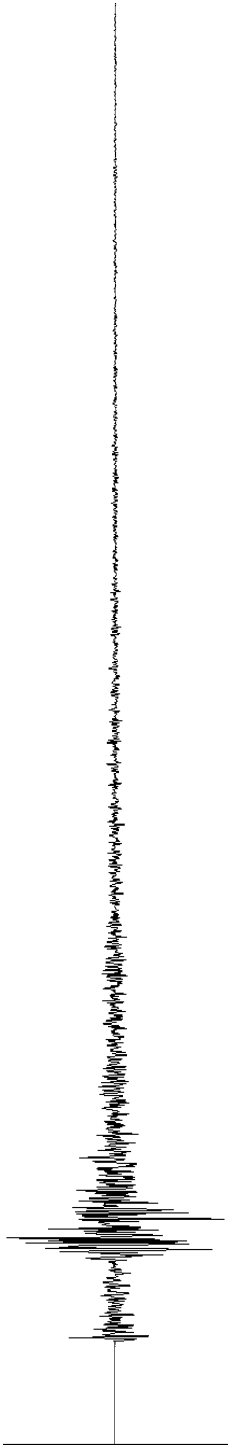


Waveform inversion

Rise times:

cannot resolve rise times smaller than minimum period contained in the data.

Synthetics for the subfault containing the hypocenter are aligned with the first significant arrival from the source region. Possible small time shifts to account for the unknown structural model (which does not take into account lateral inhomogeneities).



Waveform inversion

Objective function

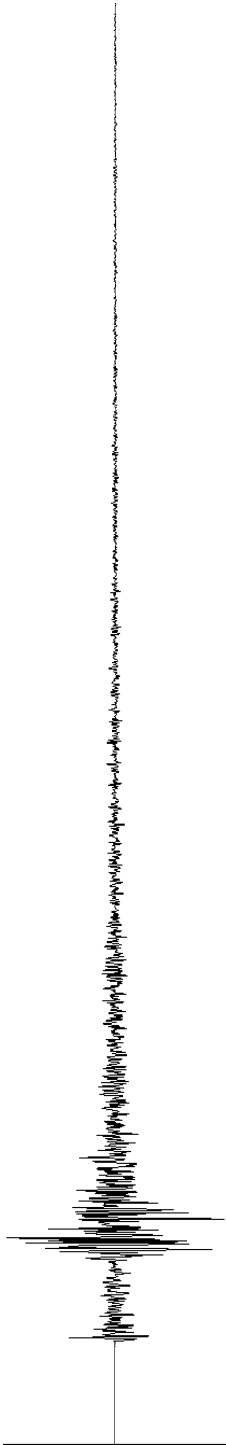
$$\sum_i W_i \int [x_i(t) - u_i(t)]^2 dt = \text{minimum}$$

with $x_i(t)$ the synthetics, $u_i(t)$ the data and W_i some weight given to the data.

This is the L2 norm, but also the L1 and other norms can be used.

Without weighting, close stations with larger seismogram amplitudes dominate the least-squares inversion (e.g. Frankel, 1992: BSSA, 82, 1511-1518).

Use several initial random models to verify that the solution is stable with respect to the starting model and inversion procedure. Important to understand what factors affect the solution.

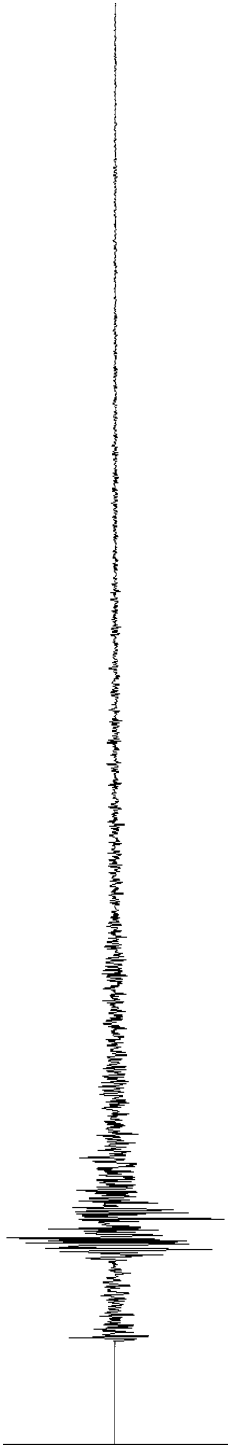


Waveform inversion

Single-window vs. multi-window inversion

Single-window inversion --> Fukuyama and Irikura, 1986
Takeo, 1987,
Beroza and Spudich, 1988:
Hartzell and Iida, 1990

In the single-window method assumes that **each point ruptures only once, when the rupture front passes**. Rupture time variations are allowed by admitting perturbations to a constant-rupture-velocity model. The perturbations are found in a separate, nonlinear inversion. Rise time is assumed to be constant and optimized by finding the value which produces the best overall fit to the data.



Waveform inversion

Multi-time-window inversion --> Olson and Apsel, 1982

Hartzell and Langer, 1993

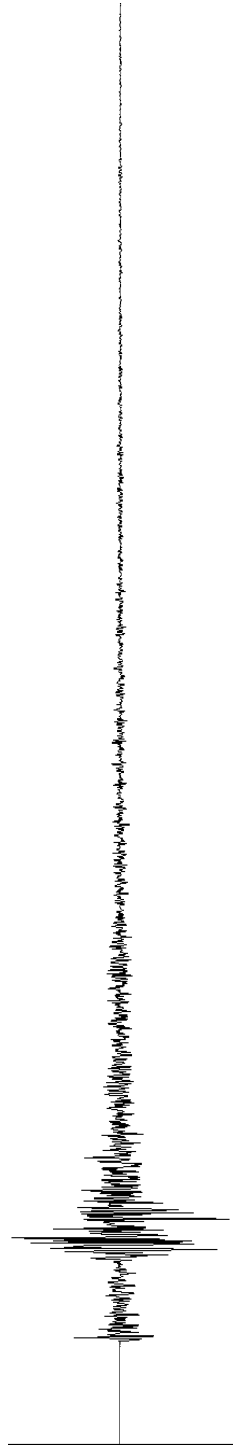
Hartzell et al. 1994

In these inversions each point on the fault is allowed to rupture multiple times.

The single-window method tends to recover the true seismic moment and the average rupture velocity.

Linear inversions with multiple-time-window tend to overestimate the moment with respect to single-time-window inversions.

Neither can resolve temporal details of the rupture propagation, unless constraints are applied (e.g. from independent data, like geodesy) .



Waveform inversion

Instability and non-uniqueness

Increasing the model dimension results in a decrease of the solution uniqueness. To stabilize the problem external constraints need to be placed on the inversion.

The parametrization itself severely restricts the possible solutions and has a big stabilizing effect.

Attention! A too restrictive parametrization can lead to the true solution lying outside the solution space of the model!

Need to parametrize the problem with sufficient flexibility to encompass realistic models of faulting:

---> **physical constraints serve to stabilize the inversion.**



Waveform inversion

Physical constraints

are desirable stabilizing tools because they can be unambiguously stated and easily adapted to reflect the current knowledge of the earthquake source physics.

Physical constraints

Positivity of slip

Strong causality (limits on rupture velocity)

Weak causality (rupture velocity smaller than P-wave velocity)

Model fits observed surface offsets

Tapering of slip to zero at the bottom of the fault

Find least moment or predetermined moment model

Model which incorporates minimum and maximum limits on rupture velocity



Waveform inversion

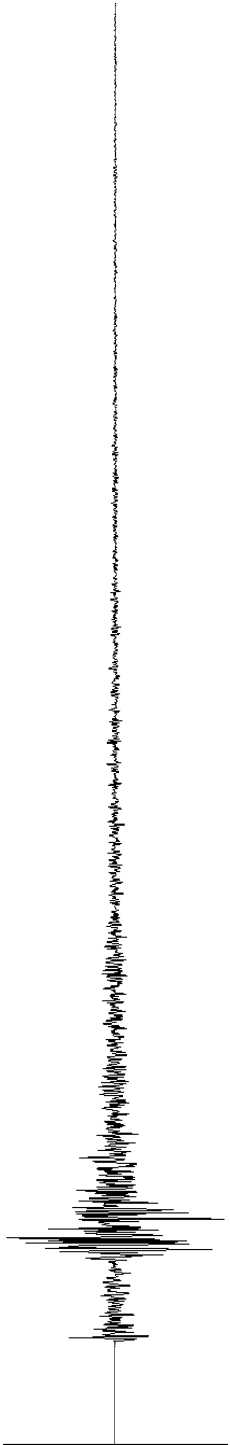
Other constraints

Find spatially smoothest model

Find minimum norm model

Incorporated as limits to the current model or as linear functions appended to the calculation of the objective function.

Some techniques require the use of several initial random models to verify that the solution is stable with respect to the starting model and inversion procedure.



Waveform inversion

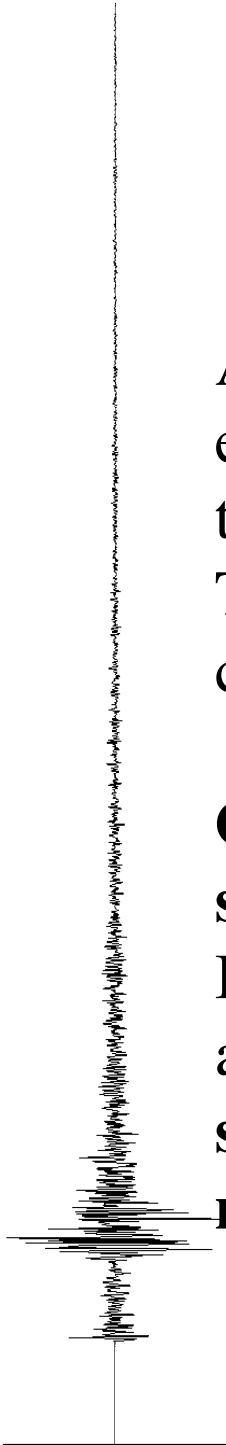
Resolution

Absolute resolution is difficult to address, because one can evaluate the resolution only for the specific problem, not for the actual earthquake source.

Therefore, usual resolution matrices are of limited value and can give only relative estimates of error.

One way is to compare solutions that utilize different data sets, parametrizations, constraints, and inversion norms.

In terms of fitting the data many solutions give an equally acceptable model. **The similarities of these different solutions are considered to be the aspects of the rupture model that are better resolved, in an absolute sense.**



Waveform inversion

Robustness

Use different methods --> the common features of these solutions point out robust characteristics of the slip distribution that are independent of the inversion parametrization.

One can use bootstrapping and jack-kniving techniques.

